Structure-Guided Minimalist Redesign of the L-Fuculose-1-Phosphate Aldolase Active Site: Expedient Synthesis of Novel Polyhydroxylated Pyrrolizidines and their Inhibitory Properties Against Glycosidases and Intestinal Disaccharidases

Xavier Garrabou,[a] Livia Gómez,[a] Jesús Joglar,[a] Sergi Gil,[b] Teodor Parella,[b] Jordi Bujons,*[a] and Pere Clapés*[a]

In memoriam to José Manuel Concellón (Universidad de Oviedo)

Abstract: A minimalist active site redesign of the L-fuculose-1-phosphate aldolase from *E. coli* FucA was envisaged, to extend its tolerance towards bulky and conformationally restricted *N*-Cbz-amino aldehyde acceptor substrates (Cbz = benzyloxycarbonyl). Various mutants at the active site of the FucA wild type were obtained and screened with seven sterically demanding *N*-Cbz-amino aldehydes including *N*-Cbz-prolinal derivatives. FucA F131A showed an aldol activity of 62 μmol h^{-1} mg^{-1} with (*R*)-*N*-Cbz-prolinal, whereas no detectable activity was observed with the FucA wild type. For the other substrates, the F131A mutant gave aldol activities from 4 to about 25 times higher than those observed with the FucA wild type. With regard to the stereochemistry of the reactions, the (*R*)-amino aldehydes gave exclusively the *anti* configured aldol adducts whereas their *S* counterparts gave variable ratios of *anti/syn* diastereoisomers. Interestingly, the F131A mutant was highly stereoselective both with (*R*)- and with (*S*)-*N*-Cbz-prolinal, exclusively producing the *anti* and *syn* aldol adducts, respectively. Molecular models suggest that this improved activity towards bulky and more rigid substrates, such as *N*-Cbz-prolinal, could arise from a better fit of the substrate into the hydrophobic pocket created by the F131A mutation, due to an additional π–cation interaction with the residue K205′ and to efficient contact between the substrate and the mechanistically important Y113′ and Y209′ residues. An expedient synthesis of novel polyhydroxylated pyrrolizidines related to the hyacinthacine and alexine types was accomplished through aldol additions of dihydroxyacetone phosphate (DHAP) to hydroxyprolinal derivatives with the hyperactive FucA F131A as catalyst. The iminocyclitols obtained were fully characterised and found to be moderate to weak inhibitors (relative to 1,4-dideoxy-1,4-imino-L-arabinitol (LAB) and 1,4-dideoxy-1,4-imino-D-arabinitol (DAB)) against glycosidases and rat intestinal saccharidases.

Keywords: aldol reaction · enzyme catalysis · inhibitors · mutagenesis · pyrrolizidines

[a] X. Garrabou, L. Gómez, Dr. J. Joglar, Dr. J. Bujons, Dr. P. Clapés
Biotransformation and Bioactive Molecules Group
Instituto de Química Avanzada de Cataluña-CSIC
Jordi Girona 18-26, 08034 Barcelona (Spain)
Fax: (+34) 932045904
E-mail: pere.clapes@iqac.csic.es

[b] S. Gil, Dr. T. Parella
Servei de Ressonància Magnètica Nuclear
Universitat Autònoma de Barcelona, Bellaterra (Spain)

Supporting information for this article is available on the WWW under http://dx.doi.org/10.1002/chem.201000714.

Introduction

Dihydroxyacetone phosphate (DHAP)-dependent aldolases are increasingly interesting biocatalysts because they catalyse stereoselective aldol additions, which are reactions of paramount importance for the synthesis of chiral polyhydroxylated structures (carbohydrates and analogues).[1] DHAP aldolases are strictly specific for the donor substrate (DHAP) and a few isosteric analogues,[2] whereas the aldehyde acceptors that they tolerate are structurally diverse.[3–5] In spite of their wide acceptor tolerance, some limitations arising from sterically demanding structures are commonly encountered. In this regard, during our ongoing research project on the aldolase-catalysed synthesis of iminocyclitols

from *N*-Cbz-amino aldehydes (Cbz = benzyloxycarbonyl), we have observed that those with α-branched substituents (i.e., isopropyl, isobutyl and *sec*-butyl), including conformationally restricted *N*-Cbz-prolinal derivatives, are poor acceptors for the FucA catalyst.[6,7] *N*-Cbz-prolinal derivatives are of particular interest for the straightforward two-step synthesis of polyhydroxylated pyrrolidines.[7]

In spite of the significant advances in the alteration of the stereospecificities of aldolases, studies focusing on modification of their acceptor substrate tolerance in the literature of chemical synthesis are rather meagre.[8] It was therefore regarded as both promising and significant to undertake a minimalist redesign of the FucA active site to extend its tolerance towards bulky and conformationally restricted acceptor substrates, while keeping the *anti* configured stereochemistry of the resulting aldol adduct.

According to the crystallographic structure of FucA reported by Schulz and co-workers,[9] it appears that the F131 and its closest residues (F206 and Y113) make up a hydrophobic wall at the binding site for the natural acceptor substrate, L-lactaldehyde. We envisaged that those residues might sterically hinder the productive binding of branched α-substituted *N*-Cbz-amino aldehydes. Moreover, the motion of the mobile C-terminal tail might also block the binding and/or prevent suitable positioning of sterically demanding aldehydes. Mutations at these positions produced relatively active catalysts towards non-natural aldehydes, although they also changed the stereochemical course of the enzymatic aldol addition reaction.[9] Strikingly, the single mutant F131A showed complete inversion of configuration for non-polar aldehydes such as propionaldehyde or isobutyraldehyde, suggesting that the side chain of F131 prevents the rotation of the aldehyde, which gives rise to the rhamnulose-like epimer. However, as has been demonstrated in previous work,[4,5] the binding modes of bulky substrates are rather unpredictable and strongly depend on the aldehyde structures, and thus their precise functional orientations in the active site during the attack of the donor. In this work we therefore pursued the investigation of two new FucA mutants, Y113A and F206A, together with the known FucA mutants F131A, Del(211–215) and Del(207–215), as well as the combination mutants F131A/F206A, Y113A/F131A and F131A/Del(207–215), as catalysts for the aldol addition reactions of DHAP to *N*-Cbz-amino aldehyde derivatives C-α substituted with isopropyl, isobutyl and *sec*-butyl groups, as well as both enantiomers of *N*-Cbz-prolinal. The F131A single mutant was then used for the straightforward stereoselective synthesis of different pyrrolidines, which were assayed as glycosidase inhibitors.

Results and Discussion

Activity of the FucA mutants on L-fuculose-1-phosphate (Fuc1P): The FucA mutants Y113A, F206A, F131A, Del-(211–215) and Del(207–215) were obtained and tested for their retroaldol activity on L-fuculose-1-phosphate (Fuc1P,

Table 1). Overall, their activities were lower than that of the wild-type enzyme.[9]

Table 1. Relative retroaldol activities of FucA mutants with L-fuculose-1-phosphate.

Aldolase	Relative specific activity[a] [%]
wild type	100
F131A	1
F206A	22
Y113A	0.5
Del(211–215)	11
Del(207–215)	2

[a] The activity of the FucA wild type was $9.8\ U\,mg^{-1}$ protein (1 U cleaves 1 μmol of Fuc1P per minute at 25 °C and pH 7.5 (Tris·HCl (100 mM) + KCl (150 mM)). Experiments were carried out in triplicate with a 5–10% estimated standard error. Mutant Y113A suffered a slow inactivation and its activity vanished during the experiment, in good agreement with the measurements on Y113F conducted by Schulz et al.[9] The rest of the mutants, F131A, Del(207–215) and Del(211–215), gave activities similar to those already reported.

Synthetic capabilities of FucA mutants: Aldol addition reactions of DHAP to *N*-Cbz-amino aldehydes, catalysed by the obtained FucA mutants, were conducted at 4 °C in DMF/buffer (1:4) with vortex mixing agitation to ensure that the aldehydes (partly soluble in water) were well dispersed in the medium.[10] The stereochemical outcomes of the enzymatic aldol addition reactions were inferred from the iminocyclitols generated after reductive amination of the corresponding aldol adducts. These iminocyclitols were structurally characterised by high-field NMR spectroscopy and by comparison of these data with those obtained for similar or identical compounds in previous work (see the Supporting Information).[4–6] In some instances the diastereomeric mixtures of non-phosphorylated aldol adducts could be directly baseline-separated by analytical reversed-phase HPLC and quantified (see the Supporting Information).

The synthetic capabilities of the FucA mutants towards (*R*)- and (*S*)-*N*-Cbz-alaninal ((*R*)-**1** and (*S*)-**1**, respectively) were first evaluated as positive blank experiments (Scheme 1). Both aldehydes were tolerated well by the FucA wild type, so their interaction with the enzyme would appear not to be subjected to any steric hindrance.[4] The F131A and F206A mutants gave comparable percentages of aldol adduct (Table 2). FucA Y113A and FucA Del(211–215) gave 24% conversions or less to aldol adducts, whereas no product was detected with Del(207–215). Importantly, the stereochemical outcome of the catalysis by the mutants was identical to that by the FucA wild type—that is, *anti*-configured products—circumstantially supporting the hypothesis that the reactive conformation of these aldehydes at the active site may differ significantly from that of the small aldehydes.[9] The initial velocities (v_o) of the FucA wild type and the F131A mutant towards (*R*)-**1** and (*S*)-**1** were measured at 25 °C. Remarkably, the v_o values of FucA F131A for (*R*)-**1** and (*S*)-**1** were between 1.5 and 3.0 times higher than those of the FucA wild type (Table 2). The change from a non-polar wall to a non-polar pocket in the
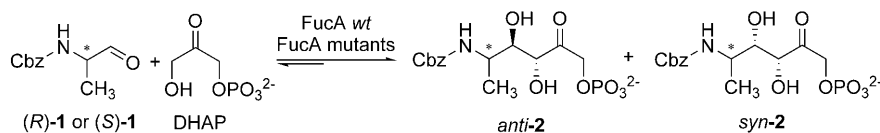
Scheme 1. FucA-catalysed aldol addition reactions of DHAP to (R)- and (S)-N-Cbz-alaninal (1); wt = wild type.

Table 2. FucA-catalysed aldol addition reactions of DHAP to (R)- and (S)-N-Cbz-alaninal ((R)-1 and (S)-1, respectively).[a]

Biocatalyst	(R)-1			(S)-1		
	%[b]	anti/syn[c]	v_o[d]	%[b]	anti/syn[c]	v_o[d]
wild type	72	100:0	12	68	100:0	23
F131A	76	98:2	37	64	99:1	36
F206A	54	99:1	n.d.	64	99:1	n.d.
Y113A	<5	n.d.[f]	n.d.	10	99:1	n.d.
Del(211–215)	24	98:2	n.d.	12	99:1	n.d.
Del(207–215)	n.p.[e]	n.d.	n.d.	n.p.	n.d.	n.d.

[a] Experiments were carried out in triplicate with an estimated standard error between 10–12%. [b] Percentage of aldol adduct 2 formed with respect to the starting DHAP (i.e., limiting substrate) after 24 h of incubation at 4°C, as determined by HPLC with use of external standards. After 24 h, no significant evolution in the product formation was detected. [c] anti/syn ratio of the biocatalytic aldol addition; syn is the (3R,4S) typical configuration obtained through catalysis by l-rhamnulose-1-phosphate aldolase from E. coli (RhuA), and anti is the (3R,4R) typical configuration obtained by FucA catalysis. [d] Initial velocities (v_o), expressed as μmol of products formed per hour and per mg of protein, were determined at 25°C. [e] No product was detected. [f] Not determined.

F131A mutant therefore created a biocatalyst with enhanced activity towards these substrates, whereas this change has a dramatic effect in the activity towards Fuc1P cleavage.[11]

The next step was to evaluate the acceptor tolerance of the FucA mutants towards the selected N-Cbz-amino aldehydes with the sterically demanding α-branched isopropyl ((R)- and (S)-3a), isobutyl ((R)- and (S)-3b) and sec-butyl ((S)-3c) substituents, as well as those ((R)- and (S)-3d) derived from (S)- and (R)-proline (Scheme 2 and Table 3).

As observed in the case of N-Cbz-alaninal, the mutants F131A and F206A gave the best levels of conversion (Table 3). In particular, F131A provided the best results for all aldehydes tested, with adduct formation twice that achieved with the FucA wild type. The most striking result was obtained with (R)-3d: F131A gave a significant percentage of aldol adduct (60%), useful at preparative scale. The results obtained with (R)- and (S)-3d prompted us to use this mutant (see below) in the preparation of novel pyrrolizidine-type iminocyclitols starting with various

N-Cbz-hydroxyprolinal acceptors.[7] The F206A mutant did not give any significant improvements in the amounts of aldol adducts formed relative to the FucA wild type except in the case of the aldehyde (R)-3d. The mutants Y113A and Del(211–215) in most cases gave <5% aldol adduct, whereas no reaction was observed with Del(207–215), consistent with the results obtained with N-Cbz-alaninal. In previous work, no aldol adduct formation had been detected (<2%) with the FucA wild type and the same aldehydes at 25°C.[6] It is noteworthy that, under the reaction conditions used in this work, the percentage of aldol adducts formed with the FucA wild type improved considerably. This difference can be accounted for, amongst other things, by two factors: firstly, by the enhanced stability of DHAP at 4°C[12] (consequently, the lower the rate of DHAP degradation the larger the conversion of acceptor that can be achieved for slow aldol addition reactions), and secondly, by the use of a vortex mixer instead of a shaker, which improved the dispersion of the aldehyde in the medium, favouring its enzymatic conversion into product. This appears to be of special relevance in reactions conducted at analytical scales.

The stereochemical outcomes of the reactions catalysed by the FucA mutants (Table 3) were governed by the structural features of the aldehydes. Within the limits of high-field NMR spectroscopy (see the Supporting Information), the R aldehydes yielded the highest anti/syn ratios (97:3 to 100:0), whereas for their S counterparts the result was dependent on the aldehyde. An interesting example that illustrates this situation was the aldolisation of (R)- and (S)-3d: with (R)-3d the reaction gave exclusively anti-5 whereas (S)-3d gave syn-5, as determined from the coupling constants and NOESY experiments performed on the unphosphorylated aldol adducts 6a and 6b, derived from (R)-3d and (S)-3d, respectively. This was also observed with the FucA wild type, however, suggesting that these mutants pre-
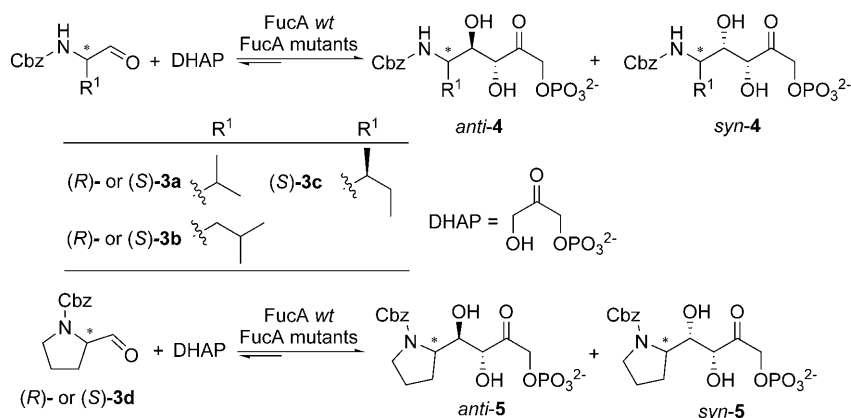
Scheme 2. FucA-catalysed aldol addition reactions of DHAP to the N-Cbz-amino aldehyde derivatives 3.

Table 3. Aldol addition reactions of DHAP to *N*-Cbz-amino aldehyde derivatives catalysed by the FucA wild type and the mutants.[a]

Biocatalyst	(R)-3a % [b]	anti/ syn [c]	(S)-3a % [b]	anti/ syn [c]	(R)-3b % [b]	anti/ syn [c]	(S)-3b % [b]	anti/ syn [c]	(S)-3c % [b]	anti/ syn [c]	(R)-3d % [b]	anti/ syn [c]	(S)-3d % [b]	anti/ syn [c]
wild type	16	100:0	16	70:30	29	100:0	27	100:0	22	78:22	2	100:0	20	0:100
F131A	56	100:0	38	45:55	68	100:0	50	85:15	36	68:32	60	97:3	39	0:100
F206A	19	100:0	12	65:35	40	100:0	24	100:0	17	74:26	10	100:0	16	0:100
Y113A	6	n.d.[d]	<5	n.d.	<5	n.d.	<5	n.d.	<5	n.d.	n.p.[e]	n.d.	n.p.	n.d.
Del(211–215)	4	n.d.	5	n.d.	8	n.d.	<5	n.d.	<5	n.d.	n.p.	n.d.	n.p.	n.d.
F131A/ F206A	21	100:0	17	65:35	34	100:0	24	85:15	24	73:27	21	100:0	14	0:100

[a] Experiments were carried out in triplicate with an estimated standard error between 10–12%. [b] Molar percentage of aldol adducts **4** and **5** formed with respect to the starting DHAP (i.e., limiting substrate) after 24 h of incubation at 4°C, as determined by HPLC with the use of external standards. No significant variation in the percentage of aldol adduct formed was detected after 24 h. [c] *anti/syn* ratio of the biocatalytic aldol addition: *syn* is the (3R,4S) typical configuration obtained by RhuA catalysis, and *anti* is the (3R,4R) typical configuration obtained by FucA catalysis. [d] n.d = not determined. [e] n.p. = no product was detected.

served the facial orientations of these aldehydes in the active site.

The initial velocities (v_o) of the FucA wild type and of FucA F131A towards (R)- and (S)-**3a**, -**3b** and -**3d** were also measured at 25°C (Table 4). Remarkably, the v_o values

Table 4. Initial reaction rates v_o (µmol h^{-1} per mg of protein) of the aldol additions of DHAP to (R)- and (S)-**3a**, -**3b** and **3d** catalysed by the FucA wild type and by FucA F131A at 25°C.

| Aldehyde | v_o [µmol h^{-1} per mg protein][a] | |
	FucA wild type	FucA F131A
(R)-**3a**	1.3	16
(S)-**3a**	3.7	14
(R)-**3b**	1.5	16
(S)-**3b**	1.8	10
(R)-**3d**	n.d.	62
(S)-**3d**	<1	25

[a] Experiments were carried out in triplicate with an estimated standard error between 10–12%. n.d. = not detected within the limits of detection by HPLC at 215 nm.

of the aldol addition reactions catalysed by FucA F131A were around 4 to 25 times higher than those of the FucA wild type. The most striking result was that obtained with (R)-**3d**: the v_o value of FucA F131A was 62 µmol h^{-1} per mg of protein, whereas the FucA wild type did not show any detectable aldol activity. Remarkably, the *anti* diastereoisomer (i.e., typically obtained with FucA catalysis) was the kinetically favoured product for both catalysts with all the aldehydes except for (S)-**3d**, for which the *syn* product (i.e., typically obtained with RhuA catalysis) was the preferred one. The stereoselectivity therefore tended to decrease as the degree of conversion or incubation time increased. This is because, under equilibrium control, more of the kinetically unfavourable product may be formed, decreasing the practical stereoselectivity of the reaction. In this context, previous molecular modelling calculations showed that the *syn* aldol adducts derived from (R)-**3a** and (S)-**3a** should be thermo-

dynamically preferred over the corresponding *anti* aldol adducts.[6] Similar calculations carried out on all the possible aldol adducts derived from (R)-**3b**, (S)-**3b**, (S)-**3c**, (R)-**3d** and (S)-**3d** confirm this trend, suggesting that the *syn* adducts are thermodynamically preferred by 4.5 kcal mol^{-1} on average (see the Supporting Information).

Double mutant—seeking for synergies: The results obtained thus far with the most successful single mutants prompted us to investigate the potential synergistic effects on the catalytic properties of combining the hyperactive F131A mutation with other modifications that would decrease the steric hindrance, thus facilitating the access of conformationally restricted aldehydes to the FucA active site. To this end, the FucA catalysts F131A/F206A, F131A/Y113A and F131A/Del(207–215) were constructed. The relative activity of F131A/F206A towards Fuc1P was approximately <0.5%, whereas no activity was displayed by the mutants FucA F131A/Y113A and FucA F131A/Del(207–215). In aldol addition reactions (Table 3), the double mutant F131A/F206A gave percentages of aldol adduct and stereoselectivities comparable to those obtained with the FucA wild type and with F206A but lower than those with the F131A mutant. No synergistic effect was therefore obtained with this FucA mutant. Furthermore, no product was detected either with the FucA F131A/Y113A or with the F131A/Del(207–215) mutants, both Y113 and the C-terminal tail residues being essential for the enzymatic aldol and retroaldol catalysis.

Retroaldol activity: The initial retroaldol rates (v_o^{retro}) of the FucA F131A, F206A and F131A/F206A mutants, as well as of the FucA wild type, were measured for the selected purified aldol adducts *anti*-(5R)-**4a**, (5S)-**4a**, *anti*-(5R)-**4b**, *anti*-(5S)-**4b** and *anti*-(5R)-**5**.[13] The purpose was to ascertain putative correlations between v_o^{retro}, the initial aldol rate (v_o) and the yields of aldol adducts achieved with the FucA mutants, particularly with F131A, relative to the FucA wild type. The initial retroaldol rates (v_o^{retro}) were assessed by continuous monitoring of the DHAP released by a multi-enzymatic test.

A cursory inspection of Table 5 reveals that, under the assay conditions, the best initial retroaldol velocities (v_o^{retro}) towards the selected substrates were achieved with the FucA F131A catalyst, in good agreement with the initial aldol rates (v_o; Tables 3 and 4), except in the case of (5S)-**4a**, for which F131A showed a slightly lower v_o^{retro} value than the wild type, probably because it was an approximately 1:1 mixture of *syn* and *anti* diastereoisomers. The most

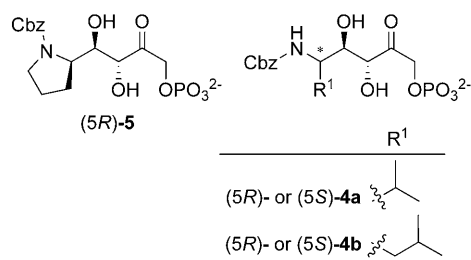**Table 5.** Initial retroaldol velocities (v_o^{retro}) of the FucA wild type and of mutants towards selected aldol adducts.

Aldol adduct	v_o^{retro} [U per mg protein][a,b]			
	FucA wild type	FucA F131A	FucA F206A	FucAF131A/ F206A
(5R)-**4a**	7.9	17	1.9	1.1
(5S)-**4a**[c]	22	17	4.3	6.2
(5R)-**4b**	12	20	6.0	1.7
(5S)-**4b**	101	244	78	40
(5R)-**5**	1.2	571	3.8	49

[a] Unit definition: 1 U will generate 1 μmol of DHAP per h at 25 °C and pH 7.5 (Tris·HCl (100 mM) + KCl (150 mM)). [b] Experiments were carried out in triplicate with an estimated standard error from 5–10 %. [c] An approximately 1:1 mixture of *syn* and *anti* diastereoisomers.

striking result was the v_o^{retro} value for the FucA F131A mutant with (5R)-**5**, which was about 500 times higher than that of the FucA wild type, showing a good correlation with the v_o values determined for the aldol addition of DHAP to (5R)-**3d**. Furthermore, the v_o^{retro} values for (5R)-**4a**, (5R)-**4b** and (5S)-**4b** were about twice as high for FucA F131A as for the FucA wild type, thus confirming the hyperactivity of this mutant towards these bulky substrates. The mutants F206A and F131A/F206A also showed higher retroaldol initial rates than the wild type towards compound (5R)-**5**, in good agreement with the higher conversions observed for the aldol additions with the aldehyde (5R)-**3d**. The retroaldol activities of the F206A and F131A/F206A mutants towards the other tested compounds were lower than those of the FucA wild type, however, whereas the levels of conversion were similar to or even higher than those achieved by the FucA wild type, indicating that there is no clear correlation between v_o^{retro} and the percentage of aldol adduct formed. This is because the aldol adducts obtained with the selected *N*-Cbz-amino aldehydes cannot form stable cyclic compounds (such as the hemiketals formed from hydroxyaldehyde acceptors), so the aldol adduct formed is always limited by reaction equilibrium. Investigations into how to overcome the thermodynamic limitation of these reactions are currently in progress in our lab.

Computational binding models: Computational modelling studies were carried out to shed light on the effects that the differential structural features of the mutant proteins obtained in this work—in particular those of the most active mutants F131A and F206A—could have on the binding

mode of the substrates, allowing for their modified catalytic properties.

To date there are a number of described FucA crystallographic structures variously of the wild-type protein or of different mutants.[9,14,15] Although the residues of the active centre are affected in many of the mutations described, the crystallographic structures show a high degree of similarity to those involving the wild type and little variation in the conformations of the other residues of this region. In all these structures there is a lack of definition of the last six to nine residues of the flexible C-terminal tail: that is, beyond residues F206–Y209 and up to residue E215. Because of the tetrameric nature of FucA, the active centre of the enzyme is made up of residues of two adjacent monomers (Figure 1), some of them belonging to the mentioned C-terminal tail of a neighbouring FucA subunit. It was therefore proposed that this flexible tail undergoes an induced fit immediately after the substrate binding at the active centre, placing residues Y209′ and E214′ within contact distance of the substrates. E73 has been suggested as the essential acid–base catalytic residue, whereas the hydroxy groups of residues Y209′ and Y113′ should be capable of establishing hydrogen bonds with the substrates (Figure 1 panel O), participating in the enzymatic mechanism by polarising the carbonyl group of the aldehyde (or the hydroxy group of the adduct) and stabilising the transition states along the aldol reaction coordinate.[9] Consistent with this role is the fact that the described Y209F and Y113F mutants show about 20-fold decreases in activity towards Fuc1P cleavage, whereas the double mutant Y113F/Y209F shows a 500-fold decrease.[9] The results obtained in this work for the Y113A mutant (Table 3) also agree with the previous observations.

Figure 1 (panel O) shows the FucA wild type active site with the modelled Y209′ and E214′ residues, together with a bound molecule of Fuc1P in which the l-lactaldehyde moiety is positioned above the DHAP portion. This illustrates the putative hydrogen-bonding interactions between the 4-OH group of Fuc1P and the phenol groups of both Y113′ and Y209′. These two residues, together with F131 and F206′, constitute a hydrophobic subsite from which a hydrophobic pocket would arise on mutation of any of them to Ala. This has been confirmed in the structure of FucA F131A,[9] which also shows that the positions of the neighbouring side chains (i.e., Y113′, K205′ and F206′) were not affected, although a higher mobility (higher B-factors) of the residues at the C-terminal end was apparent. It is therefore plausible that the hydrophobic phenyl group from the Cbz moiety of aldol adducts could be located in the pocket generated by the F131A or F206A mutations.

Accordingly, the structures for the complexes of FucA F131A, FucA F206A and FucA wild type with the *anti* aldol adduct from (R)-**3d** (that is, (3R,4R,5R)-**5**) and the *syn* adduct from (S)-**3d** (that is, (3R,4S,5S)-**5**) were modelled as shown in Figure 1 (Panels A to F). The stability of the binding modes shown in Figure 1 was further assessed by running short restrained molecular dynamics (MD) under implicit solvent conditions (see the Supporting Information).
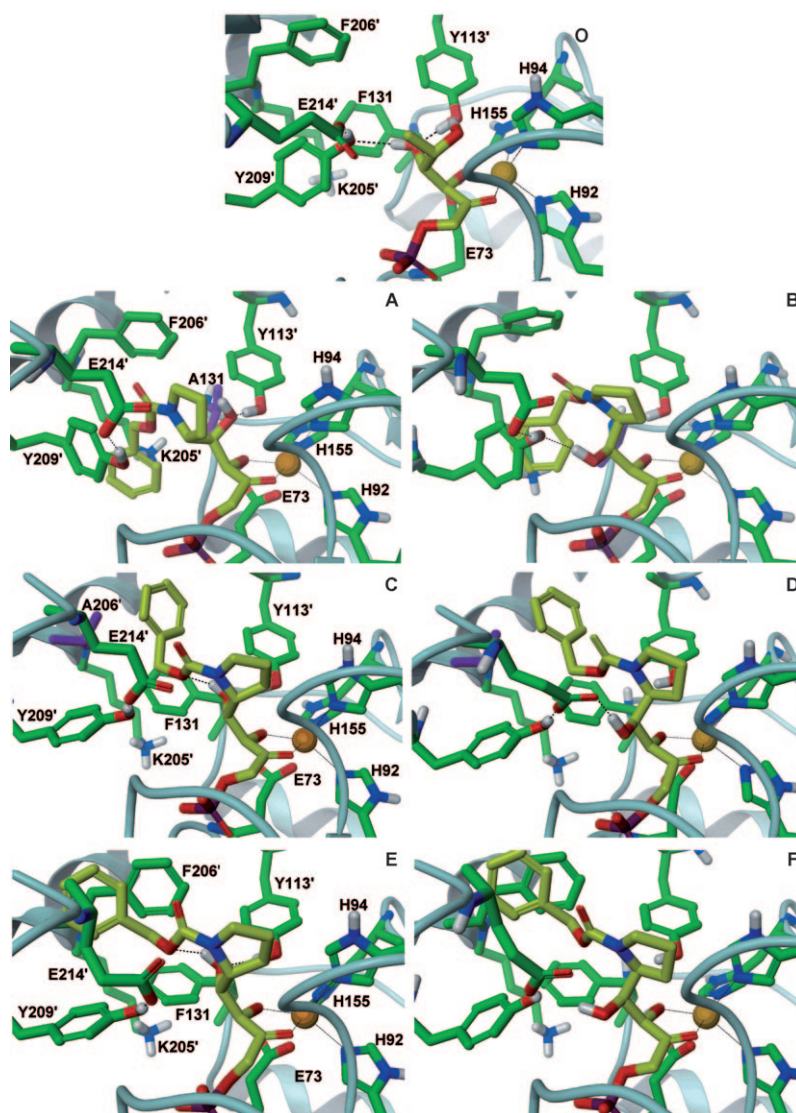
Figure 1. Modelled Fuc1P bound to the active centre of the FucA wild type (panel O). A prime in the number-ing (Y113′, for example) denotes a residue from a neighbouring FucA subunit. The model includes a possible 3D arrangement for the residues of the C-terminal tail, based on a previous model by Joerger et al.[9] Energy-minimised models of the *anti*-aldol adduct from (*R*)-**3d** (panels A, C and E) and the *syn*-aldol adduct from (*S*)-**3d** (panels B, D and F) bound into the active sites of FucA F131A (panels A and B), FucA F206A (pan-els C and D) and FucA wild type (panels E and F). The mutated residues are highlighted in violet.

tion of the Cbz-phenyl group is apparently stabilised by a π–cation interaction with the charged ε-amine group of the K205′ residue (i.e., shortest dis-tance between the nitrogen of the ε-amine of K205′ and the carbon atoms of the Cbz-phenyl ring in any of the complexes is 3.0–3.2 Å), which is maintained after the MD runs (see the Sup-porting Information). This in-teraction would increase the binding affinity of these sub-strates for the active site of the F131A mutant relative to the FucA wild type and FucA F206A, because such interac-tion would be precluded as a result of the presence of the F131 residue in those proteins. Indeed, whereas in the F206A mutant the Cbz-phenyl ring may be efficiently accommodat-ed in the cavity left by the mu-tation, the models for the FucA wild type complexes (Figure 1, E and F) suggest that to occupy an analogous position parallel to the aromatic side chain of F206′, the phenyl group of Cbz would have to force the side chain of Y209′ to shift away from the position that it occu-pies in the structure of the un-bound protein. Further reloca-tion of the aromatic rings of Cbz and Y209′ is observed during the MD runs, indicating that the smaller volume of the active site cavity on FucA wild type would give rise to steric clashes with the substrate.

From these structures, it is noteworthy that the *anti* adduct can establish a hydrogen bond interaction between its reac-tive 4-OH group and the phenol group of residue Y113′ in all complexes, whereas the *syn* adduct can do the same with residues Y209′ or E214′. These interactions are mostly main-tained during the MD trajectory, suggesting that they could efficiently participate in the enzyme mechanism as previous-ly described. Moreover, it appears that the phenyl group from Cbz can occupy the pockets generated by the F131A and F206A mutations, as would be expected (Figure 1, A/B and C/D, respectively), with the proline ring occupying a po-sition above the DHAP moiety similar to the arrangement of the L-lactaldehyde moiety on bound Fuc1P (Figure 1 panel O). Furthermore, for the F131A complexes the loca-

Therefore, although alternative binding modes could be suggested, these models appear to correlate well with the observed hyperactivity shown by the F131A mutant towards the aldehydes (*R*)-**3d** and (*S*)-**3d** (Table 4) or the (5*R*)-**5** *anti* adduct (Table 5). Moreover, similar binding modes could also be expected for the substrates **3a**, **3b**, **4a** and **4b**, which would yield higher affinities of these substrates relative to the FucA wild type, due to the stabilisation arising from the π–cation interaction with the K205′ residue. Consequently, this could also translate into the generally higher activities towards those substrates shown in Tables 4 and 5 for the F131A mutant. Mutant F206A had less sharply differenti-ated activities relative to the wild-type enzyme (Tables 3 and 5), which would appear consistent with the fact that the

models did not show a significantly improved binding mode for the mutant other than the better accommodation of the bulky Cbz moiety in the pocket generated by the mutation. This probably explains the slightly better activity observed towards the (5R)-**5** *anti* adduct, whereas for the rest of the substrates this effect might be compensated by their lower conformational restriction, which could favour better accommodation of the substrates in the active site of the FucA wild type.

Synthetic application—a concise synthesis of pyrrolidine-type iminocyclitols: The high activity of FucA F131A towards *N*-Cbz-proline aldehyde derivatives prompted us to explore its ability to catalyse aldol additions of DHAP to hydroxyproline derivatives as acceptors for the preparation of various polyhydroxylated pyrrolidine iminocyclitols related to the hyacinthacine and alexine families (for papers on polyhydroxylated pyrrolidine synthesis see[16–23]). Interestingly, some of these bicyclic iminocyclitols are inhibitors of intestinal saccharidases,[24–27] with potential applications as adjuvants for the treatment of non-insulin-dependent diabetes mellitus and for the prevention and control of obesity.[28] To this end, *cis*-4-hydroxy-(R)-Cbz-prolinal ((2R)-**7a**), *trans*-4-hydroxy-(S)-Cbz-prolinal ((2S)-**7b**) and *trans*-3-hydroxy-(S)-Cbz-prolinal ((2S)-**7c**) were assayed as acceptors for the FucA F131A aldolisation with DHAP (Scheme 3) to produce the aldol adducts **8** in good yields (Table 6).
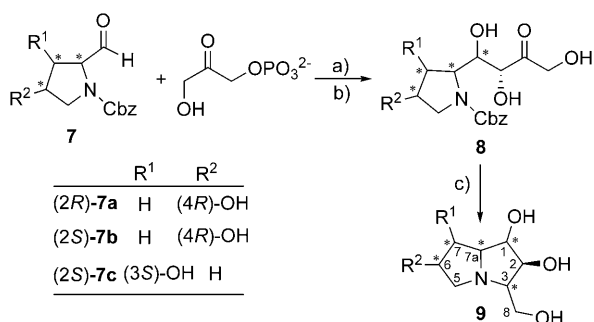
Scheme 3. FucA F131A-catalysed aldol additions of DHAP to *N*-Cbz-prolinal derivatives for the synthesis of polyhydroxylated pyrrolidine derivatives. a) FucA F131A, b) acid phosphatase, c) H$_2$ (50 psi), Pd/C.

Within the limits of high-field NMR spectroscopy (see below and in the Supporting Information), the aldol additions catalysed by FucA F131A were fully stereoselective. Analogously with the aldehydes (R)-**3d** and (S)-**3d**, (2R)-**7a** provided the corresponding *anti* (3R,4R) adduct, whereas with (2S)-**7b** and (2S)-**7c** both aldolases gave *syn* (that is, (3R,4S) RhuA stereochemistry) adducts.

The aldol adducts **6a** and **8a**–**8c** were subjected to reductive amination (Scheme 4) by the procedure already described by us.[7] The crude materials obtained were purified by cation exchange chromatography[7] and the products were structurally characterised by NMR spectroscopy (Table 7, see below and the Supporting Information). From

Table 6. FucA F131A-catalysed aldol additions of DHAP to *N*-Cbz-prolinal derivatives. Reaction productivity and isolated yields of the corresponding synthesised aldol adducts

Aldehyde	%[a]/*t* [h]	Yield[b] [%]	Product
(R)-**3d**	71/24	33	**6a**
(S)-**3d**	68/24	52	**6b**[c]
(2R)-**7a**	95/24	60	**8a**
(2S)-**7b**	87/48	49	**8b**
(2S)-**7c**	76/48	44	**8c**

[a] Molar percentages of phosphorylated aldol adducts **6a**–**8c** formed, based on the starting DHAP (i.e., limiting substrate) as determined by HPLC with external standards. Reaction conditions described in the Experimental Section. [b] Yield of the isolated product, purification procedures were not optimised. [c] Product identical to the one obtained by RhuA catalyst and isolated in a previous study.[7]

the stereochemistry at C3, it can be concluded that the reductive amination with Pd was fully stereoselective for **8b** and moderately so ($\approx$3:1) for the rest of the compounds. For the aldol adducts **6a**, **6b**, **8b** and **8c** the major diastereomers formed were those with *syn* 1-OH/3-CH$_2$OH configurations, as observed in other reductive aminations,[4–6] whereas for **8a** the contrary was true. Interestingly, the unexpected pyrrolidine **9g** was isolated; it was probably formed catalytically (i.e., formal H$_2$O elimination/hydrogenation) during the Cbz removal/reductive amination step. Compounds **9a** and **9d**–**g** were obtained and characterised for the first time in this work. The syntheses of compound **9h** and its enantiomer have been reported by Koch et al.[21] and Behr et al.,[22] respectively. The chemical synthesis of **9b**, that is, 7a-*epi*-hyacinthacine A1, has recently been reported.[29] Compound **9i** was isolated from the seeds of *Castanospermum australe* with [α]$_D^{22}$ = +11.6 (c = 0.37 in H$_2$O),[25] but the absolute stereochemistry could not be determined. Compound **9i** synthesised in this work had [α]$_D^{22}$ = +17.9 (c = 1.7 in H$_2$O). Due to the internal reference of the specific absolute configuration introduced by the two chiral centres of aldehyde (S)-**7c**, compound **9i** as described here corresponds with compound number **10** reported by Nash et al.[25]

NMR spectroscopy analysis of proline derivatives: The unphosphorylated aldol adducts **6a**, **6b** and **8a**–**8c**, as well as **6c** from a previous study involving RhuA,[7] were structurally characterised by NMR spectroscopy (see the Supporting Information). Room-temperature ^{1}H NMR spectra of all these compounds show broad signals, so low-temperature NMR spectroscopy experiments (250 K) were required for full characterisation. Each spectrum corresponds to two
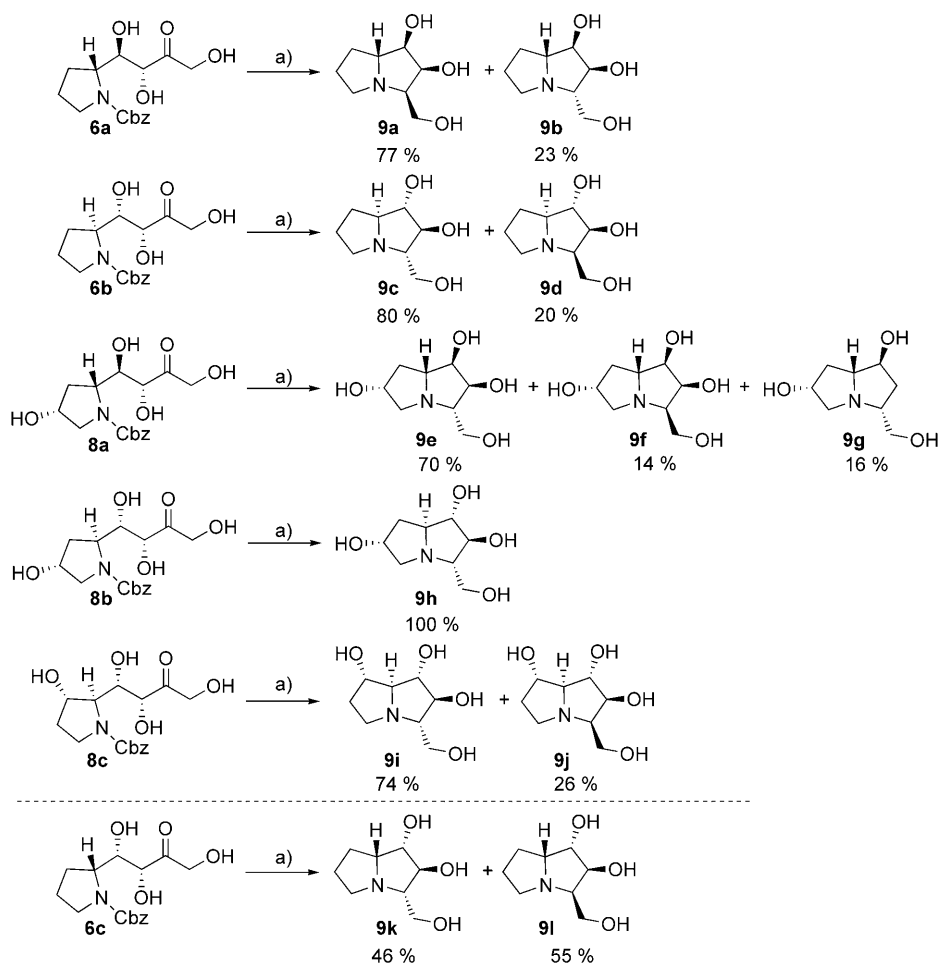
Scheme 4. Reductive amination of the aldol adducts **6a–6b** and **8a–8d** and the products identified after purification. a) H₂, Pd/C). Aldol adduct **6b** and pyrrolizidines **9c** and **9d** were also obtained with use of the RhuA catalyst.[7] For purposes of comparison, the aldol adduct **6c** and the pyrrolizidines **9k** and **9l** were taken from a previous study with RhuA catalyst.[7] Compounds **9d** and **9l** are the correctly assigned products from the previous study (see compounds **7** and **9**, respectively, from the paper of Calveras et al.[7]).

Ref. [7]). Two of them were stereochemically assigned by NMR spectroscopy as 1*S*,2*S*,3*S*,7a*S* (**6**) and 1*S*,2*S*,3*S*,7a*R* (**8**), as typically generated from RhuA catalysis, and two more to 1*R*,2*S*,3*R*,7a*S* (**7**) and 1*R*,2*S*,3*R*,7a*R* (**9**), epimeric at C1 and C3, typically from FucA catalysis. In the light of those results, it was concluded that RhuA aldolase was not stereoselective. Through assessment of the NMR spectra data for the pyrrolizidine iminocyclitols derived from the (*R*)-**3d** and (*S*)-**3d** aldehydes reported in our previous study[7] and comparison with those obtained in this work, it can be confirmed unequivocally that the aldol additions of DHAP to proline derivatives catalysed by RhuA and FucA aldolases were fully stereoselective (see the Supporting Information). The pyrrolizidine iminocyclitol structures, that is, the products numbered **7** and **9** in the previous study,[7] were hence incorrectly assigned at their C1 stereocentres: as 1*R*,2*S*,3*R*,7a*S* and 1*R*,2*S*,3*R*,7a*R* instead of the correct **1S**,2*S*,3*R*,7a*S* and **1S**,2*S*,3*R*,7a*R*, respectively. Therefore, the pertinent conclusion, consistent with the results of this paper, is that for most of the proline-derived adducts the reductive amination by Pd was not stereoselective and gave mixtures of two diastereoisomers epimeric at C3.

main conformations, which was also corroborated by computational calculations (see the Supporting Information). From the NMR spectroscopy data, within the limits of detection, the enzymic aldol addition reactions of DHAP to (*R*)-**3d** and (*S*)-**3d** were fully stereoselective and single *anti* or *syn* diastereoisomers were obtained (see the Supporting Information).

The hyacinthacine and alexine analogues were also structurally characterised and their relative stereochemistries were unequivocally assigned by NMR spectroscopy. Basically, the relative configurations of the different C1, C2, C3 and C7a stereocentres can be determined by the concerted use of NOE enhancements and *J*(H,H) coupling constants (see Table 7 and the Supporting Information). As a general trend, all pyrrolizidine derivatives show a *cis* conformation between the nitrogen lone pair and H7a, in close agreement with theoretical calculations.
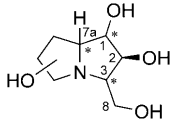
In a previous study, we demonstrated that RhuA was able to accommodate (*R*)-**3d** and (*S*)-**3d** to give four stereoisomers of hyacinthacines A1 and A2 (compounds **6–9** in

Inhibitory activity against glycosidases: The polyhydroxylated pyrrolizidines generated were screened as inhibitors against a panel of commercially available glycosidases (Table 8) and rat intestinal disaccharidases (sucrase, lactase, threalase and maltase, Table 9). For purposes of comparison, the inhibitory activities of the previously synthesised iminocyclitols 1,4-dideoxy-1,4-imino-L-arabinitol (LAB, **10a**), 1,4-dideoxy-1,4-imino-D-arabinitol (DAB, **10b**), D-fagomine (**11a**) and L-fagomine (**11b**) and of the pyrrolizidines **9k** and **9l** were also evaluated.[4,5,7] Both **10a** and **10b** had inhibitory properties consistent with those previously published.[32] Interestingly, LAB showed moderate inhibitory activity towards α-L-rhamnosidase and no inhibition towards α-D-mannosidase and α-L-fucosidase, whereas the contrary was true for DAB. Compound **11a** was found to be a weak inhibitor of α-D-glucosidase from rice,[33] whereas its enan-

Table 7. ^{1}H/^{13}C chemical shifts (ppm) and ^3J(H,H) coupling constants for compounds **9a–9l** (in D$_2$O)

Compound[a]	H1 (C1)	H2 (C2)	H3 (C3)	H7a (C7a)	^3J(7a,1)	^3J(1,2)	^3J(2,3)
9a	3.89 (79.3)	4.23 (75.7)	2.93 (71.1)	3.37 (69.3)	8.5	3.8	3.5
9b	4.00 (76.9)	4.09 (72.6)	3.42 (66.6)	3.63 (73.0)	2.3	5.1	10.2
9c[b]	3.74 (79.0)	3.78 (82.1)	2.75 (71.4)	3.20 (68.3)	8.0	8.0	9.5
9d[b,c]	3.96 (83.7)	4.10 (81.8)	3.38 (67.1)	3.37 (74.8)	2.2	1.6	3.8
9e	4.01 (77.9)	4.14 (72.8)	3.19 (67.1)	3.40 (70.1)	2.9	5.4	9.1
9f	4.39 (79.6)	4.31 (75.3)	3.56 (73.4)	3.74 (69.8)	8.9	3.4	3.4
9g	4.30 (78.3)	1.86–2.12 (35.6)	3.71 (65.2)	3.63 (75.1)	≈0	5.5; ≈0	4.7; 12.5
9h	3.87 (82.7)	3.85 (80.0)	2.82 (72.5)	3.45 (67.8)	7.3	7.0	8.5
9i	3.71 (80.1)	3.76 (78.6)	2.69 (70.8)	3.04 (76.4)	8.2	8.2	8.8
9j	4.17 (81.2)	4.17 (81.2)	3.44 (67.4)	3.23 (80.4)	2.0	2.0	6.8
9k[b]	4.15 (78.3)	3.92 (77.6)	3.20 (66.6)	3.82 (66.9)	7.8	6.4	9.3
9l[b,c]	4.05 (77.5)	4.31 (80.8)	3.04 (70.8)	3.83 (69.5)	4.4	1.5	3.6

[a] Compounds of this work and references to others with identical relative stereochemistry at C1, C2, C3, and C7a: **9a** and **9f**,[19,27] **9b** and **9e**,[29,30] **9c**, **9h** and **9i**,[20,22,26,27,31] **9d** and **9j**,[17] **9k**,[18,22] **9l**[27] [b] Data from a previous study.[7] [c] **9d** and **9l** are the correctly assigned products from the previous study (see compounds **7** and **9**, respectively, from the paper of Calveras et al.[7]).

10a **10b** **11a** **11b**
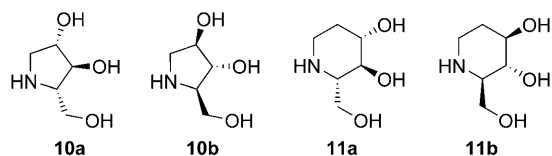
tiomer **11b** had poorer inhibitory properties against α-D-glucosidase from rice but elicited some activity against β-D-galactosidase from bovine liver. A cursory inspection of Table 8 reveals that, of the glycosidases tested, the polyhydroxylated pyrrolizidines were active and selective against α-D-glucosidase from rice, with the most potent being **9c**,[7] with a configuration at C1, C2, C3 and C7a identical to that of LAB. The presence of hydroxy groups at C6 (**9h**) or C7 (**9i**) or inversion of the C7a stereocentre (**12**) decreased K_i values and produced weaker inhibitors. Remarkably, **9a** was a potent inhibitor of α-L-rhamnosidase from *P. decumbens* with a K_i value about 10 times lower than that of **12** with inverted C1 and C3 stereocentres, and much lower than those of **13** and **9b**, with inversion only at C1 or C3. Compound **9a** was also a moderate inhibitor of α-L-fucosidase and the most potent of those synthesised in this work towards this glycosidase. Interestingly, the presence of a hydroxy group at C6 (**9f**) and the lack of the hydroxy at C2 (**9g**) dramati-

cally decreased the inhibitory activity towards α-L-fucosidase.

Inhibitory activity against rat intestinal disaccharidases: It has been reported that polyhydroxylated pyrrolizidines are inhibitors of rat intestinal disaccharidases,[24–27] so we also screened the synthesised pyrrolizidines **9a–9j** as inhibitors of these. For purposes of comparison, LAB (**10a**), DAB (**10b**), D-fagomine (**11a**) and L-fagomine (**11b**) were also included. The two compounds **10a** and **10b** were the most active against the rat intestinal saccharidases, consistently with the reported literature values (Table 9),[32] whereas **11a** and **11b** were poor inhibitors of sucrase and maltase. Of the polyhydroxylated pyrrolizidines of this work, **9h** was the most active against sucrase, lactase and, particularly, maltase. Compound **9h** has the same configuration as **10a** at C1, C2 and C3. Changing the hydroxy group from the C6 to the C7 position (compound **9i**) completely removed its inhibitory properties against disaccharidases. Moreover, inversion of the stereochemistry of C3 in **9i** (compound **9j**) resulted in recovery of some activity. The introduction of a hydroxy group at C6 and/or elimination of the hydroxy group at C2 in **9a** (compounds **9f** and **9g**, respectively, for example) also abolished the inhibitory properties. Changing the C3 configuration in **9f** (compound **9e**, for example) did not have any effect on the inhibitory properties. Overall, none of the pyrrolizidines synthesised showed any remarkable inhibition of the disaccharidases assayed.

Conclusion

Minimal changes in the FucA active site, for example FucA F131A and FucA F206A, lead to new aldolase mutants with improved tolerance towards sterically demanding C-α substituted N-Cbz-amino aldehydes. FucA F131A was a hyperactive mutant that showed the best synthetic capabilities with regard to the conformationally restricted N-Cbz-prolinal derivatives. The double mutant FucA F131A/F206A did not improve on the results achieved with one single mutation, so there was no synergism of these two mutations. Measurements of retroaldol activities towards the *anti* (3R,4R) adducts showed that FucA F131A was the most

Table 8. Activities (IC$_{50}$ (μM) and K_i (μM) values (in parentheses)) of the synthesised compounds against commercially available glycosidases.[a]

Compound	α-D-Glucosidase[f]	α-D-Glucosidase[j]	β-D-Glucosidase[k]	β-D-Galactosidase[l]	α-L-Rhamnosidase[m]	α-D-Mannosidase[n]	α-L-Fucosidase[o]
10a[b]	1.8 ± 0.1 (0.8 ± 0.1)[g]	0.05 ± 0.01 (0.04 ± 0.01)[i]	685 ± 112 (1014 ± 81)[i]	n.i.	56 ± 5 (98 ± 5)[g]	n.i.	n.i.
10b[c]	0.33 ± 0.02 (0.17 ± 0.01)[h]	61 ± 7 (104 ± 75)[h]	276 ± 25 (100 ± 64)[h]	n.i.	n.i.	286 ± 27 (111 ± 60)[i]	20 ± 1 (5 ± 1)[h]
11a[d]	n.i.[q]	61 ± 7 (18 ± 8)[h]	n.i.	n.i.	n.i.	n.i.	n.i.
11b[c]	n.i.	126 ± 7 (236 ± 61)[h]	n.i.	154 ± 22 (76 ± 21)[h]	n.i.	n.i.	n.i.
9a	n.i.	n.i.	n.i.	n.i.	2.0 ± 0.2 (2.1 ± 0.8)[i]	n.i.	185 ± 9 (18 ± 6)[i]
9b	n.i.	804 ± 7	n.i.	n.i.	422 ± 12 (340 ± 35)[g]	n.i.	264 ± 18 (143 ± 33)[h]
9c[e]	n.d.[r]	30 (4.7 ± 0.5)[h]	n.i.	n.i.	115 (57.0 ± 0.9)[h]	n.i.	n.i.
9d[e,p]	n.d.	700	n.i.	n.i.	n.i.	n.i.	n.i.
9e	n.i.	271 ± 138 (357 ± 110)[h]	n.i.	n.i.	n.i.	n.i.	n.i.
9f	n.i.	n.i.	n.i.	n.i.	598 ± 78 (478 ± 80)[h]	n.i.	n.i.
9g	n.i.	690 ± 287 (411 ± 16)[h]	n.i.	n.i.	n.i.	n.i.	620 ± 45
9h	n.i.	44 ± 9 (25 ± 3)[h]	448 ± 60 (555 ± 202)[g]	447 ± 22 (688 ± 200)[g]	n.i.	174 ± 97 (149 ± 19)[h]	n.i.
9i	n.i.	72 ± 22 (311 ± 23)[h]	n.i.	n.i.	196 ± 31 (221 ± 9)[h]	95 ± 41 (600 ± 8)[h]	327 ± 7 (100 ± 4)[h]
9j	n.i.	31 ± 11 (477 ± 91)[h]	n.i.	n.i.	n.i.	n.i.	n.i.
9k[d]	n.d.	800	n.i.	n.i.	90 (33 ± 1)[g]	n.i.	n.i.
9l[d,p]	n.d.	n.i.	n.i.	n.i.	300	n.i.	n.i.

[a] Data are the mean values of triplicate experiments ± standard error of the mean (SE). [b] Synthesised in a previous work.[5] [c] Synthesised in a previous work.[34] [d] Synthesised in a previous work.[35] [e] Inhibitory data taken from ref. [7]. [f] From baker's yeast. [g] Noncompetitive inhibition ($\alpha = 1$). [h] Competitive inhibition. [i] Noncompetitive inhibition ($\alpha \neq 1$).[36] [j] From rice. [k] From sweet almonds. [l] From bovine liver. [m] From *Penicillium decumbens*. [n] From jack beans, *Genus Canavalia*. [o] From bovine kidney. [p] Structures assigned incorrectly at C1 stereocentre in our previous study.[7] [q] n.i. = no inhibition: that is, IC$_{50} \geq 1$ mM. [r] n.d. = not determined.

Table 9. Activities (IC$_{50}$ (μM)) of the synthesised compounds against rat intestinal saccharidases.[a]

Compound	Sucrase	Lactase	Trehalase	Maltase
10a	0.29 ± 0.02	50 ± 36	74 ± 34	0.2 ± 0.1
10b	22 ± 12	140 ± 84	67 ± 19	50 ± 36
11a	484 ± 4	n.i.[b]	n.i.	209 ± 92
11b	144 ± 26	n.i.	n.i.	n.i.
9a	179 ± 56	n.i.	n.i.	n.i.
9b	463 ± 202	n.i.	n.i.	n.i.
9h	138 ± 12	196 ± 12	n.i.	88 ± 8
9j	142 ± 55	n.i.	224 ± 54	n.i.
activity (UI)[c]	4.01 ± 0.48	0.75 ± 0.07	2.44 ± 0.41	27.50 ± 3.55

[a] The experiments were performed in triplicate for each set of saccharidases obtained from one rat. Two different rats ($n = 2$) were used. Activities are expressed as μM ± standard error of the mean (SE). [b] n.i. = no inhibition, that is, IC$_{50} \geq 1$ mM. [c] Activity of each intestinal saccharidase towards their natural substrate, that is, sucrose, lactose, threhalose and maltose, respectively.

active, in good agreement with its initial velocity (v_o) values for the aldol addition reactions. Remarkably, the mutant F131A and the double mutant F131A/F206A gave initial retroaldol rates with the aldol adduct from (R)-prolinal around 500- and 40-times higher, respectively, than that of the FucA wild type. In addition, FucA F131A showed activity improvements, relative to the rest of the substrates, of around 4- to >25-fold in the aldol addition and up to 2.4-fold in the retroaldol reactions. On the other hand, it was observed that the initial retroaldol velocities of the F206A and F131A/F206A mutants were lower than those of the FucA wild type, whereas the contrary was true for the percentages of aldol adducts formed. However, it must be taken into account that the aldol adducts obtained with the selected N-Cbz-amino aldehydes cannot form stable cyclic compounds, so the amount of aldol adduct formed is always limited by the reaction equilibrium. The reaction yield may therefore not be directly predicted from the retroaldol activities and other factors, including those relating to the precise mechanisms for the aldol and retroaldol reactions and how they affect the kinetics and the reaction equilibrium, must be considered.

Molecular models suggest that the improved activity of FucA F131A towards bulky and more rigid substrates, such as N-Cbz-prolinal, could be the result of improved affinity of the substrate for the active centre of the enzyme due to an additional π–cation interaction with the K205′ residue

and of the efficient contact between the substrate and the mechanistically important Y113′ and Y209′ residues.

FucA F131A was used as a catalyst for the aldol addition reactions of DHAP to *N*-Cbz-hydroxyprolinal derivatives, allowing a concise synthesis of novel polyhydroxylated pyrrolizidines of the hyacinthacine and alexine types. These new iminocyclitol derivatives showed moderate activities against α-D-glucosidase from rice and low activities against rat intestinal sucrase. Among them, compound **9a** was a potent inhibitor of α-L-rhamnosidase from *P. decumbens* and a moderate inhibitor of α-L-fucosidase from bovine kidney and **9h** was moderately active against sucrase, lactase and maltase rat intestinal disaccharidases.

Experimental Section

Materials: Synthetic oligonucleotides were purchased from MWG-Biotech. Acid phosphatase (PA, EC 3.1.3.2, 5.3 U mg^{-1}) was from Sigma–Aldrich. The precursor of dihydroxyacetone phosphate (DHAP), dihydroxyacetone phosphate dimer bis(ethyl ketal), was synthesised in our lab by a procedure described by Jung et al.[37] with slight modifications. Deionised water was used for preparative HPLC and Milli-Q-grade water for analytical HPLC. All other solvents used were of analytical grade. Individual enantiomerically pure *N*-Cbz-amino aldehydes used in this study were synthesised in our lab by previously published procedures.[6] The dicyclohexylamine salt of l-fuculose-1-phosphate (Fuc1P) was synthesised with the use of FucA aldolase as described in reported procedures.[38] Glycerol 3-phosphate dehydrogenase from rabbit muscle (GDH) and NADH were from Sigma–Aldrich. The plasmid pQE-FucA containing the gene for expression of His-tagged l-fuculose-1-phosphate aldolase was a generous gift from the Departament d'Enginyeria Química of the Universitat Autònoma de Barcelona.[39] High density IDA agarose 6BCL (nickel charged) was from Hispanagar.

HPLC analyses: HPLC analyses were performed with a RP-HPLC cartridge (250×4 mm) filled with Lichrosphere 100 (RP-18, 5 μm) from Merck (Darmstadt, Germany). Samples (25 μL) were withdrawn from the aldol reactions, dissolved in MeOH (1 mL) to stop the reaction and analysed by HPLC. The solvent system used was: solvent A (aqueous trifluoroacetic acid (TFA) (0.1%, v/v)) and solvent B (TFA (0.095%, v/v) in acetonitrile/H$_2$O 4:1), gradient elution from 10 to 70% B (reactions with aldehydes (*R*)-**1** and (*S*)-**1**) or 30 to 90% B (reactions with aldehydes (*R*)- and (*S*)-**3a**, -**3b**, -**3c** and -**3d**) over 30 min, flow rate 1 mL min^{-1}, detection 215 nm, column temperature 30°C. The amounts of aldol adduct produced were quantified from the peak areas by use of an external standard methodology. The external standards consisted of solutions of purified aldol adducts of known concentration.

Electrospray mass spectrometry of proteins: *Sample preparation*: Each protein (1 mL of (NH$_4$)$_2$SO$_4$ suspension) was centrifuged and resuspended in water (1 mL). Samples were dialysed against water (5 L, 0.1% formic acid) to remove the salts. Samples (10 μL) were analysed by HPLC-ESI-MS with use of an Acquity UPLC BEH300 C18 column (1.7 μm, 2.1×100 mm) and an ESI-TOF mass spectrometer (LCT PremierWaters, Milford, MA, USA) fitted with a 4 GHz time-to-digital converter (TDC) with a dual ESI source (LockSpray). The second sprayer provided the lock mass calibration with leucine enkephalin (*m/z* 556.2771). The ESI-TOF was operated in the W-optics mode, thus providing a mass resolution of at least 10 000 full-width at half maximum (FWHM). The acquisition time per spectrum was set to 0.2 s, and the mass range was from 500 to 1800 Da. Data were acquired with use of a cone voltage of 50 V, a capillary voltage of 3000 V, a desolvation temperature of 350°C, and a source temperature of 100°C. The desolvation gas flow was set at 400 L h^{-1} and the cone gas flow was set at 30 L h^{-1}. The solvent system used for the elution was: solvent A (aqueous formic acid (0.1%, v/v)) and solvent B (formic acid (0.1%, v/v) in acetonitrile), gradi-

ent elution 0% B for 5 min, from 5 to 70% B over 12 min, from 70 to 100% B over 1 min, flow rate 0.3 mL min^{-1}. MassLynx 4.1 (Waters, Milford, MA, USA) was used for data acquisition and processing. Magtran software,[40] kindly provided by Dr. Zhongqi Zhang (Amgen, Inc., Thousand Oaks, CA), was used for molecular weight deconvolution from ESI-MS spectra of proteins.

Mutagenesis: FucA gene mutations were introduced with the aid of the QuikChange site-directed mutagenesis kit (Stratagene), with the oligonucleotides listed in the Supporting Information and the plasmid pQE-FucA as template. DNA sequencing and mass spectra analysis of the expressed proteins (see the Supporting Information) confirmed the expected mutations in the gene sequence.

Gene expression and protein purification: For protein production, the plasmids were transformed into *E. coli* strain M-15 [pREP-4] (QIAGEN). Cells were grown at 37°C in 2 L flasks containing defined medium (1 L) with ampicillin (100 mg L^{-1}) and kanamycin (25 mg L^{-1}), up to an optical density of 0.6 at 600 nm.[41] At that point, protein expression was induced by addition of isopropyl β-D-thiogalactoside (IPTG) to a final concentration of 50 μM and the temperature was lowered to 30°C to avoid formation of inclusion bodies. After an additional 4 h of incubation, cells were harvested, suspended in starting buffer (disodium hydrogen phosphate (50 mM), NaCl (300 mM), imidazole (20 mM), pH 8.0) and lysed by use of a Cell Disrupter (TS 0.75 kW 40 K, Constant Systems). Cellular debris was removed by centrifugation at 12 000 g for 10 min. The clear supernatant was collected and purified by affinity chromatography in a FPLC system (Amersham Biosciences). The crude supernatant was applied to a cooled HR 16/40 column (GE Healthcare) containing affinity beads (50 mL) and was washed with start buffer (150 mL). The protein was eluted with disodium hydrogen phosphate buffer (pH 8.0, 50 mM) containing NaCl (300 mM) and imidazole (300 mM) at a flow rate of 3 mL min^{-1}. ZnSO$_4$ (up to 1 mM) was added to the eluted protein and the mixture was incubated for 15 min. Addition of (NH$_4$)$_2$SO$_4$ (0.4 g mL^{-1} of liquid) caused protein precipitation. The resulting pellet was centrifuged at 12 000 g for 10 min, suspended in (NH$_4$)$_2$SO$_4$ (50 mL, 0.4 g mL^{-1}) and centrifuged again. The pellet was finally suspended in (NH$_4$)$_2$SO$_4$ (50 mL, 0.4 g mL^{-1}) and stored at 4°C.

Analytical methods: Protein concentration was calculated by colour densitometry in SDS-PAGE with use of Image J 1.37 v. Activity assays with the natural substrate l-fuculose-1-phosphate were carried out as described by Durany et al.[42]

Initial aldol velocity: The initial aldol velocities (v_o) were determined by measuring the amount of aldol adduct produced by HPLC at the initial reaction times. The *N*-Cbz-amino aldehyde (24.5 μmol) was dissolved in dimethylformamide (72 μL) and mixed with freshly neutralised (pH 6.9) DHAP solution (141 μL, 14.4 μmol). The aldolase solution (100 μL, 0.29 mg, amount corresponding to 8 U mL^{-1} reaction for the FucA wild type) was added to this mixture, which was placed in a vortex mixer (1000 rpm) at 25°C. Samples (25 μL) were withdrawn at different times (7, 15, 30 and 60 min) and diluted with MeOH (500 μL), and the amount of aldol adduct produced was analysed and quantified by HPLC as described above. Linear correlations were found for levels of conversion lower than 15%. The estimated standard error for three determinations was between 10–12%.

Initial retroaldol velocity: Retroaldol assays with the aldol adducts (*R*)-**5** and (*R*)- and (*S*)-**4a** and -**4b** were carried out by the previous assay method with some modifications. A solution of NADH (2 mM) in Tris·HCl buffer (pH 7.5, 100 mM, 0.9 mL) containing KCl (150 mM), the aldolase (variable amount depending on the activity) and glycerol-3-phosphate dehydrogenase (1.7 U mL^{-1}) was incubated at 25°C for 5 min. The corresponding aldol adduct (100 μL, 100 mM) in Tris·HCl buffer (pH 7.5, 100 mM) containing KCl (150 mM) was added to this solution up to a total final volume of 1 mL. The decrease in the absorbance of NADH at 340 nm was measured.

Enzymatic aldol reactions: Analytical scale reactions (360 μL total volume) were conducted in 2 mL test tubes stirred with a vortex mixer (VIBRAX VXR basic, Ika) at 1500 rpm and 4°C. The *N*-Cbz-amino aldehyde (24.5 μmol) dissolved in dimethylformamide (72 μL) was mixed with freshly neutralised (pH 6.9) DHAP solution (141 μL, 14.4 μmol).

The mixture was cooled on ice, the aldolase solution (100 μL, 0.29 mg, amount corresponding to 8 U mL⁻¹ reaction for the FucA wild type) was added to start the aldol reaction, and the reactor was placed in a vortex mixer (1000 rpm) at 4 °C. At 24 h samples (25 μL) were withdrawn, diluted with MeOH (1.0 mL) and analysed by HPLC under the conditions described above.

Preparative enzymatic aldol addition reactions (15–20 mL total volume) were conducted to obtain the corresponding iminocyclitols and thus to infer the stereoselectivity of the enzymatic aldol addition reaction. The procedures utilised were similar to those described by us in previously reported work.[6,43] The stereochemistry of the resulting iminocyclitols was unequivocally assessed by comparison of their high-field NMR spectroscopy data with compounds previously obtained and fully characterised in our lab (see the Supporting Information).[4,6,43]

The aldol adducts **6a** and **6b** were also directly characterised by NMR spectroscopy (see below and the Supporting Information) to determine the relative configurations of the two newly formed stereogenic centres. For purposes of comparison the unphosphorylated aldol adducts with *syn* configurations of the vicinal diols, obtained from the aldol additions of DHAP to (*R*)-**3d** and (*S*)-**3d** catalysed by L-rhamnulose-1-phosphate aldolase from *E. coli*,[7] were also characterised in this work by NMR spectroscopy (see the Supporting Information).

Preparative synthesis of polyhydroxylated pyrrolizidine derivatives from proline analogues: The syntheses of the *N*-Cbz-hydroxy prolinal derivatives (*R*)-**7a**, (*S*)-**7b** and (*S*)-**7c** were easily achievable from the corresponding commercial *cis*-4-hydroxy-(*R*)-proline, *trans*-4-hydroxy-(*S*)-proline, and *trans*-3-hydroxy-(*S*)-proline. As an example the procedure for the synthesis of *trans*-*N*-Cbz-3-hydroxy-(*S*)-prolinal ((*S*)-**7c**) is described.

a) *trans*-3-Hydroxy-(*S*)-proline methyl ester hydrochloride: *trans*-3-Hydroxy-(*S*)-proline (5.0 g, 38.1 mmol) was dissolved in MeOH (20 mL) and the mixture was cooled to 0 °C with an ice bath. SO₂Cl₂ (76.3 mmol, 5.56 mL) was added to this solution dropwise at such a rate as to maintain the reaction mixture below 4 °C. Stirring of the reaction mixture was continued at room temperature overnight. The solvent was then removed under reduced pressure and the obtained solid was washed with ethyl ether (6.8 g, 98 %).

b) *trans*-3-*N*-Cbz-Hydroxy-(*S*)-proline methyl ester: The methyl ester hydrochloride derivative (6.8 g, 37.5 mmol) and bicarbonate (119 mmol, 10 g) were dissolved in dioxane/water 1:1 (50 mL). *N*-(Benzyloxycarbonyl)succinimide (37.5 mmol, 9.3 g) dissolved in dioxane was then added dropwise over 1 hour. After 24 h the solvent was removed under vacuum, and the crude product was dissolved with ethyl acetate and washed with citric acid (10 %, 3×200 mL), bicarbonate (3×200 mL) and brine (2×200 mL). The organic layer was dried over anhydrous Na₂SO₄ and dried to obtain an oil (10.3 g, 98 %).

c) *trans*-3-*N*-Cbz-Hydroxy-(*S*)-prolinol: The *N*-Cbz-hydroxy proline methyl ester derivative (10.3 g, 36.9 mmol) was reduced by treatment with NaBH₄ (147.5 mmol, 5.6 g) by the same procedure as described by Luly et al. (Method B) with a slight modification.[44] After the addition of NaBH₄ the reaction was allowed to warm up slowly to room temperature.

d) *trans*-3-*N*-Cbz-Hydroxy-(*S*)-prolinal ((*S*)-7c): The *N*-Cbz-hydroxy prolinol (1.0 g, 4.0 mmol) was oxidised by treatment with 2-iodoxybenzoic acid (IBX) by the procedures already described by us.[6,7] Complex NMR spectra due to the presence of multiple rotamers were recorded.

***cis*-4-Hydroxy-(*R*)-Cbz-prolinal ((*R*)-7a)**: The title compound was prepared by the General Procedure described above (0.83 g, 84 %). [α]$_D^{22}$= +19.5 (*c*=1.9 in CH₃OH); ¹H NMR (500 MHz, CDCl₃): δ=9.74 (s, 0.5H), 9.66 (s, 0.5H), 7.40 (m, 5H), 5.31–5.00 (m, 2H), 4.50–4.00 (m, 2H), 3.81–3.38 (m, 2H), 2.94–2.13 ppm (m, 2H); ¹³C NMR (101 MHz, CDCl₃): δ=199.7, 199.5, 155.8, 155.0, 136.4, 136.1, 128.9, 128.8, 128.8, 128.6, 128.5, 128.3, 128.2, 70.3, 69.4, 67.9, 67.8, 63.8, 63.7, 56.0, 55.2, 36.3, 35.5 ppm.

***trans*-4-Hydroxy-(*S*)-Cbz-prolinal ((*S*)-7b])**: The title compound was prepared by the General Procedure described above (0.88 g, 89 %). [α]$_D^{22}$= −38.5 (*c*=2.5 in CH₃OH); ¹H NMR (500 MHz, CDCl₃): δ=9.61 (d, ³*J*= 1.9 Hz, 0.5H), 9.48 (d, ³*J*=3.1 Hz, 0.5H), 7.53–7.24 (m, 5H), 5.34–5.05

(m, 2H), 4.64–4.18 (m, 1H), 4.01–3.19 (m, 3H), 3.11–1.62 ppm (m, 2H); ¹³C NMR (101 MHz, CDCl₃): δ=199.7, 199.5, 155.8, 155.0, 136.4, 136.1, 128.9, 128.8, 128.8, 128.6, 128.5, 128.3, 128.2, 70.3, 69.4, 67.8, 67.8, 63.8, 63.7, 56.0, 55.2, 36.3, 35.5 ppm.

***trans*-3-Hydroxy-(*S*)-Cbz-prolinal ((*S*)-7c)**: The title compound was prepared by the General Procedure described above (0.81 g, 82 %). [α]$_D^{22}$= −58.6 (*c*=3.2 in CH₃OH); ¹H NMR (500 MHz, CDCl₃): δ=9.63 (s, 0.5H), 9.55 (d, ³*J*=1.2 Hz, 0.5H), 7.46–7.30 (m, 5H), 5.39–4.99 (m, 2H), 4.61–4.19 (m, 1H), 4.11–2.94 (m, 3H), 2.67–1.54 ppm (m, 2H); ¹³C NMR (101 MHz, CDCl₃): δ=199.2, 155.8, 154.9, 136.4, 136.3, 128.8, 128.4, 128.2, 74.0, 73.5, 72.8, 71.5, 67.7, 45.2, 44.9, 33.2, 32.6 ppm.

Enzymatic aldol condensations (General Procedure): Reactions at preparative scale (20–40 mL total volume) were performed in 50 mL Erlenmeyer flasks with screw caps. The *N*-Cbz-prolinal derivative (1.7–3.4 mmol, 1.7 equiv per mol DHAP) was dissolved in DMF (the amount corresponding to 20 %, v/v of the total). The DHAP solution (volume corresponding to 80 %, v/v of the total, 1–2 mmol) at pH 6.9, freshly prepared as described above, was then added dropwise with stirring at 4 °C, with a vortex mixer. Finally, FucA F131A (0.8–1.3 mg per mL reaction mixture) was added and mixed again. The Erlenmeyer was placed on a horizontal shaking bath (200 rpm) at 4 °C. The reactions were monitored by HPLC. When the amount of aldol adduct was constant with the time (24 h) the reaction was stopped by addition of MeOH (1.5 times the reaction volume). The methanol was then evaporated off and the aqueous solution was washed with ethyl acetate to remove the unreacted *N*-protected amino aldehyde. The aqueous layer was collected, the remaining ethyl acetate was removed under reduced pressure, and the product was lyophilised. The solid obtained was dissolved in plain water (ca 10–20 mL) and the pH was adjusted to 5.5 with TFA. Acid phosphatase (5.3 U per mmol phosphorylated adduct) was added to this solution. The reaction was followed by HPLC until no starting material was detected. Further phosphatase units were added, if necessary, to direct the reaction to completion. The reaction mixture was then filtered through a 0.45 μm cellulose membrane filter. The filtrate was loaded onto a XTerra (19× 250 mm) column, and eluted with a gradient of CH₃CN (8 to 56 % over 30 min) in plain water. Pure fractions were pooled and lyophilised.

These products were structurally characterised by NMR spectroscopy with special attention to the elucidation of the relative configurations of the newly formed stereogenic centres. The specific chiral centres of the starting *N*-Cbz-prolinals served as internal references for the assignment of the absolute stereochemistry for the new formed ones. Because these were intermediates no further physical data were determined.

(*R*)-Benzyloxycarbonyl-2-((1*R*,2*R*)-1,2,4-trihydroxy-3-oxobutyl)pyrrolidine (6a): The title compound was prepared by the General Procedure described above (194 mg, 33 %). Major conformation ¹H NMR (500 MHz, CD₃OD, 250 K): δ=7.33–7.46 (m, 5H), 5.15–5.10 (m, 2H), 4.58 (A of AB system, ³*J*=19.0 Hz, 1H), 4.43 (B of AB system, ³*J*= 19.1 Hz, 1H), 4.24 (dd, ³*J*=7.8, 3.3 Hz, 1H), 4.11 (m, 1H), 4.08 (d, ³*J*= 7.8 Hz, 1H), 3.55 (m, 2H), 2.12 (m, 1H), 2.02 (m, 1H), 1.92 (m, 1H), 1.82 ppm (m, 1H); ¹³C NMR (101 MHz, CD₃OD, 250 K): δ=212.2, 156.8, 138.0–129.6, 76.9, 71.9, 68.0, 67.7, 60.8, 48.3, 25.8, 25.5 ppm. Minor conformation ¹H NMR (500 MHz, CD₃OD, 250 K): δ=7.33–7.46 (m, 5H), 5.21–5.15 (m, 2H), 4.55 (A of AB system, ³*J*=19.1 Hz, 1H), 4.35 (B of AB system, ³*J*=19.2 Hz, 1Hm, 1H), 4.08 (dd, ³*J*=8.8, 1.9 Hz, 1H), 4.19 (m, 1H), 4.01 (d, ³*J*=7.8 Hz, 1H), 3.55 (m, 2H), 2.15 (m, 1H), 2.02 (m, 1H), 1.96 (m, 1H), 1.82 ppm (m, 1H); ¹³C NMR (101 MHz, CD₃OD, 250 K): δ=212.2, 156.6, 138.0–129.6, 76.2, 72.8, 67.9, 67.7, 60.3, 48.4, 26.0, 25.1 ppm.

(*S*)-Benzyloxycarbonyl-2-((1*S*,2*R*)-1,2,4-trihydroxy-3-oxobutyl)pyrrolidine (6b): The title compound was prepared by the General Procedure described above (167 mg, 52 %). Major conformation ¹H NMR (500 MHz, CD₃OD, 250 K): δ=7.34–7.48 (m, 5H), 5.18–5.18 (m, 2H), 4.61 (A of AB system, ³*J*=20.0 Hz, 1H), 4.51 (B of AB system, ³*J*=19.9 Hz, 1H), 4.18 (d, *J*=1.6 Hz, 1H), 3.98 (m, 1H), 3.81 (dd, ³*J*=1.6, 8.7 Hz, 1H), 3.47 (m, 2H), 2.17–1.95 (m, 2H), 1.95 ppm (m, 2H); ¹³C NMR (101 MHz, CD₃OD, 250 K): δ=213.7, 158.6, 138.2–129.2, 77.8, 73.5, 68.4, 68.2, 60.4, 47.7, 27.9, 24.3 ppm. Minor conformation ¹H NMR (500 MHz, CD₃OD, 250 K): δ=7.48–7.34 (m, 5H), 5.21–5.13 (m, 2H), 4.53 (A of AB system,

$^3J = 19.8$ Hz, 1H), 4.40 (B of AB system, $J = 19.7$ Hz, 1H), 4.23 (dd, $^3J =$ 2.4, 3.3 Hz, 1H), 4.15 (d, $^3J = 2.4$ Hz, 1H), 4.03 (m, 1H), 3.54–3.43 (m, 2H), 2.35–2.01 (m, 2H), 1.98–1.82 ppm (m, 2H); ^{13}C NMR (101 MHz, CD$_3$OD): $\delta = 213.7$, 158.6, 138.2–129.5, 78.7, 73.6, 68.4, 68.2, 61.4, 47.7, 27.5, 24.8 ppm.

(R)-Benzyloxycarbonyl-2-((1R,2R)-1,2,4-trihydroxy-3-oxobutyl)-4-(R)-hydroxypyrrolidine (8 a): The title compound was prepared by the General Procedure described above (204 mg, 60%). Major conformation ^{1}H NMR (600 MHz, CD$_3$OD): $\delta = 7.39$ (m, 5H), 5.15–5.12 (m, 2H), 4.59 (A of AB system, $^3J = 19.3$ Hz, 1H), 4.45 (B of AB system, $^3J = 19.3$ Hz, 1H), 4.33 (d, $^3J = 2.3$ Hz, 1H), 4.30 (m, 1H), 4.26 (br s, 1H), 4.10 (d, $^3J =$ 8.1 Hz, 1H), 3.70 (m, 1H), 3.33 (m, 1H), 2.17 ppm (m, 1H); ^{13}C NMR (101 MHz, CD$_3$OD): $\delta = 210.6$, 155.4, 129.2–138.2, 75.4, 69.2, 68.3, 66.7, 66.5, 58.9, 55.2, 32.5 ppm. Minor conformation ^{1}H NMR (600 MHz, CD$_3$OD): $\delta = 7.39$ (m, 5H), 5.22–5.17 (m, 2H), 4.54 (A of AB system, $^3J = 19.3$, 95.7 Hz, 1H), 4.38 (B of AB system, $^3J = 19.4$, 95.6 Hz, 1H), 4.32 (m, 1H), 4.33 (m, 1H), 4.32 (m, 1H), 4.22 (d, $^3J = 1.4$ Hz, 1H), 4.05 (d, $J = 8.4$ Hz, 1H), 3.70 (m, 1H), 3.29 (m, 1H), 2.26 ppm (m, 1H); ^{13}C NMR (101 MHz, CD$_3$OD): $\delta = 210.7$, 155.3, 129.5–138.2, 75.0, 70.4, 69.5, 66.7, 66.5, 58.5, 55.4, 33.1 ppm.

(S)-Benzyloxycarbonyl-2-((1S,2R)-1,2,4-trihydroxy-3-oxobutyl)-4-(R)-hydroxypyrrolidine (8 b): The title compound was prepared by the General Procedure described above (251 mg, 49%). Major conformation ^{1}H NMR (600 MHz, CD$_3$OD): $\delta = 7.39$ (m, 5H), 5.17–5.17 (m, 2H), 4.59 (A of AB system, $^3J = 19.7$, 1H), 4.51 (B of AB system, $^3J = 19.6$ Hz, 1H), 4.39 (s, 1H), 4.39 (m, 1H), 4.23 (d, $^3J = 4.9$ Hz, 1H), 4.19 (m, 1H), 4.14 (m, 1H), 3.63 (d, $^3J = 11.9$ Hz, 1H), 3.42 (dd, $^3J = 11.6$, 4.2 Hz, 1H), 2.32 (m, 1H), 2.03 ppm (m, 1H); ^{13}C NMR (101 MHz, CD$_3$OD): δ 213.7, 129.2–138.2, 158.6, 77.0, 71.8, 69.3, 67.0, 66.4, 59.1, 54.3, 34.8 ppm. Minor conformation ^{1}H NMR (600 MHz, CD$_3$OD): $\delta = 7.39$ (m, 5H), 5.24–5.11 (m, 2H), 4.48 (A of AB system, $^3J = 19.5$ Hz, 1H), 4.34 (B of AB system, $^3J = 19.6$ Hz, 1H), 4.46 (m, 1H), 4.39 (br s, 1H), 4.14 (m, 1H), 4.11 (d, $^3J = 2.5$ Hz, 1H), 3.62 (d, $^3J = 11.9$ Hz, 1H), 3.48 (dd, $^3J = 11.9$, 3.8 Hz, 1H), 3.36 (m, 1H), 2.47 (m, 1H), 1.99 ppm (m, 1H); ^{13}C NMR (101 MHz, CD$_3$OD): $\delta = 213.7$, 158.6, 129.5–138.2, 77.3, 71.0, 69.3, 67.0, 66.0, 59.1, 54.9, 34.0 ppm.

(S)-Benzyloxycarbonyl-2-((1S,2R)-1,2,4-trihydroxy-3-oxobutyl)-3-(S)-hydroxypyrrolidine (8 c): The title compound was prepared by the General Procedure described above (149 mg, 44%). ^{1}H NMR (600 MHz, CD$_3$OD): $\delta = 7.41$ (m, 5H), 5.19 (m, 2H), 4.62 (A of AB system, $^3J =$ 20.0 Hz, 1H), 4.52 (B of AB system, $^3J = 19.8$ Hz, 1H), 4.48 (br s, 1H), 4.17 (s, 1H), 3.85 (d, $^3J = 9.5$ Hz, 1H), 3.66 (d, $^3J = 9.3$ Hz, 1H), 3.64 (m, 1H), 3.52 (t, $^3J = 9.9$ Hz, 1H), 2.18 (tt, $^3J = 13.5$, 6.6 Hz, 1H), 1.94 ppm (dd, $^3J = 13.7$, 7.0 Hz, 1H); ^{13}C NMR (101 MHz, CD$_3$OD): $\delta = 211.9$, 157.7, 129.2–138.2, 76.2, 71.5, 72.0, 67.5, 67.3, 67.0, 44.9, 31.0 ppm.

Removal of Cbz group and reductive amination: The aldol adducts obtained (0.40–0.74 mmol) were dissolved in ethanol (5–10 mL), followed by the addition of plain water (20–45 mL). Pd/C (200 mg) was added. The reaction mixture was shaken under hydrogen (50 psi) overnight at room temperature. After removal of the catalyst by filtration through deactivated aluminium oxide, the pH of the filtrate was adjusted to pH 5.5 with formic acid (1 M), the solvent was removed under reduced pressure, and the product was lyophilised.

Purification by ion exchange chromatography: The polyhydroxylated pyrrolizidine derivatives 9a, 9b and 9e–9j were separated by ion exchange chromatography with a FPLC system by a procedure described by us.[6,7] CM-Sepharose CL-6B (Amersham Pharmacia) in NH$_4$$^+$ form stationary phase was packed into a glass column (450×25 mm) to provide a final bed volume of 220 mL. The flow rate was 4 mL min^{-1}. The CM-Shepharose-NH$_4$$^+$ was washed initially with H$_2$O. An aqueous solution of the crude material at pH 7 was then loaded onto the column. Minor coloured impurities were washed away with H$_2$O (150 mL, 3 bed volumes). The retained compounds were eluted with aqueous NH$_4$OH (0.01 M): compounds 9a and 9b (load 150 mg), 9a (elution volume, 584 mL, 51 mg), 9b (elution volume, 992 mL, 15 mg); compounds 9e–9g: 9e (elution volume 260 mL, 17 mg), 9f (elution volume 376 mL, 3 mg), 9f (elution volume 512 mL, 4 mg); compound 9c (elution volume 376 mL, 49 mg); compounds 9g and 9h: 9g (elution volume 416 mL, 10 mg), 9h (elution

volume 48 mL, 26 mg). In each case, when necessary the operation was repeated until the whole of the crude sample was consumed. Pure fractions were pooled and lyophilised. Physical and NMR spectroscopy data are listed below. ^{1}H and ^{13}C NMR spectra assignments are given in the Supporting Information.

(1R,2S,3R,7aR)-1,2-Dihydroxy-3-(hydroxymethyl)pyrrolizidine (2-epihyacinthacine A2, 9a): The title compound was prepared by the General Procedure described above (51 mg, 49% from the aldol adduct). $[\alpha]_D^{22} =$ -26.5 ($c = 2$ in H$_2$O); ^{1}H NMR (500 MHz, D$_2$O): $\delta = 4.23$ (t, $^3J = 3.6$ Hz, 1H), 3.89 (dd, $^3J = 8.7$, 3.9 Hz, 1H), 3.83 (dd, $^3J = 11.0$, 7.7 Hz, 1H), 3.64 (dt, $^3J = 12.4$, 6.2 Hz, 1H), 3.37 (td, $^3J = 8.3$, 3.6 Hz, 1H), 2.93 (ddd, $^3J =$ 7.9, 6.2, 3.3 Hz, 1H), 2.84 (m, 1H), 2.70 (dt, $^3J = 11.0$, 5.6 Hz, 1H), 1.92 (m, 1H), 1.83 (m, 1H), 1.76 ppm (m, 2H); ^{13}C NMR (101 MHz, D$_2$O): $\delta = 79.4$, 75.9, 71.3, 66.2, 62.6, 56.7, 31.7, 26.9 ppm. ESI-TOF: m/z calcd for C$_8$H$_{16}$NO$_3$ $[M+H]^+$: 174.1130; found 174.1131.

(1R,2S,3S,7aR)-1,2-Dihydroxy-3-(hydroxymethyl)pyrrolizidine (9b): The title compound was prepared by the General Procedure described above (15 mg, 14% from the aldol adduct). $[\alpha]_D^{22} = -45.3$ ($c = 1.5$ in H$_2$O); ^{1}H NMR (500 MHz, D$_2$O): $\delta = 4.08$ (dd, $^3J = 4.9$, 10.0 Hz, 1H), 4.00 (dd, $^3J = 5.0$, 1.8 Hz, 1H), 3.91 (m, 2H), 3.63 (td, $^3J = 8.5$, 1.7 Hz, 1H), 3.41 (ddd, $^3J = 10.0$, 8.5, 4.5 Hz, 1H), 3.13 (m, 1H), 2.91 (td, $^3J = 10.7$, 5.7 Hz, 1H), 2.25 (m, 1H), 1.99 (m, 1H), 1.73 (m, 1H), 1.58 ppm (m, 1H); ^{13}C NMR (101 MHz, D$_2$O): $\delta = 77.3$, 72.8, 72.7, 66.7, 61.3, 50.0, 31.6, 28.0 ppm. ESI-TOF: m/z calcd for C$_8$H$_{16}$NO$_3$ $[M+H]^+$: 174.1130; found 174.1132.

(1R,2S,3S,6R,7aR)-1,2,6-Trihydroxy-3-(hydroxymethyl)pyrrolizine (9e): The title compound was prepared by the General Procedure described above (17 mg, 15% from the aldol adduct). $[\alpha]_D^{22} = -39.6$ ($c = 1.3$ in H$_2$O); ^{1}H NMR (500 MHz, D$_2$O): $\delta = 4.32$ (m, 1H), 4.13 (dd, $^3J = 9.3$, 5.4 Hz, 1H), 4.01 (dd, $^3J = 5.3$, 2.7 Hz, 1H), 3.86 (m, 2H), 3.41 (td, $^3J =$ 8.0, 2.5 Hz, 1H), 3.18 (m, 1H), 3.07 (A of AB system, $^3J = 9.6$, 5.8 Hz, 1H), 2.70 (B of AB system, $^3J = 9.4$, 8.0 Hz, 1H), 2.44 (m, 1H), 1.58 ppm (dt, $^3J = 12.9$, 7.8 Hz, 1H); ^{13}C NMR (101 MHz, D$_2$O): $\delta = 77.9$, 73.0, 72.8, 70.7, 67.2, 61.8, 55.2, 39.2 ppm; ESI-TOF: m/z calcd for C$_8$H$_{16}$NO$_4$ $[M+H]^+$: 190.1079; found 190.1077.

(1S,2S,3R,7S,7aS)-1,2,7-trihydroxy-3-(hydroxymethyl)pyrrolizine (9 f): The title compound was prepared by the General Procedure described above (3 mg, 3% from the aldol adduct). ^{1}H NMR (500 MHz, D$_2$O): $\delta =$ 4.57 (s, 1H), 4.39 (dd, $^3J = 8.7$, 3.8 Hz, 1H), 4.31 (t, $^3J = 3.3$ Hz, 1H), 3.91 (A of AB system, $^3J = 11.6$, 6.2 Hz, 2H), 3.81 (B of AB system, $^3J = 11.7$, 7.2 Hz, 1H), 3.75 (m, 1H), 3.57 (m, 1H), 3.25 (A of AB system, $^3J = 12.5$, 3.1 Hz, 1H), 3.12 (B of AB system, $^3J = 12.1$ Hz, 1H), 2.26 (m, 1H), 2.04 ppm (d, $^3J = 13.6$ Hz, 1H); ^{13}C NMR (101 MHz, D$_2$O): $\delta = 79.6$, 75.3, 75.2, 73.3, 69.8, 62.9, 61.7, 38.5 ppm; ESI-TOF: m/z calcd for $[M+H]^+$ C$_8$H$_{16}$NO$_4$: 190.1079; found 190.1076.

(1S,3R,6R,7aR)-1,6-Dihydroxy-3-(hydroxymethyl)pyrrolizine (9g): The title compound was prepared by the General Procedure described above (4 mg, 4% from the aldol adduct). $[\alpha]_D^{22} = -22.2$ ($c = 0.09$ in H$_2$O); ^{1}H NMR (500 MHz, D$_2$O): $\delta = 4.37$ (m, 1H), 4.30 (d, $^3J = 5.4$ Hz, 1H), 3.85 (A of AB system, $^3J = 12.3$, 5.2, 1H), 3.80 (B of AB system, $^3J = 12.3$, 8.1 Hz, 1H), 3.71 (s, 1H), 3.64 (m, 1H), 3.20 (d, $^3J = 8.2$ Hz, 1H), 2.79 (t, $^3J = 9.1$ Hz, 1H), 2.52 (m, 1H), 2.13 (td, $^3J = 13.1$, 5.4, 1H), 1.87 (m, 1H), 1.59 ppm (dt, $^3J = 13.3$, 8.1 Hz, 1H); ^{13}C NMR (101 MHz, D$_2$O): $\delta = 77.7$, 75.6, 71.9, 65.8, 61.7, 53.9, 38.6, 35.4 ppm; ESI-TOF: m/z calcd for $[M+H]^+$ C$_8$H$_{16}$NO$_3$: 174.1130; found 174.1126.

(1S,2S,3S,6R,7aS)-1,2,6-Trihydroxy-3-(hydroxymethyl)pyrrolizine (9h): The title compound was prepared by the General Procedure described above (49 mg, 35% from the aldol adduct). $[\alpha]_D^{20} = -21.0$ ($c = 1.4$ in H$_2$O) [lit. (enantiomer)[22] $[\alpha]_D^{20} = +16.0$ ($c = 0.2$ in H$_2$O); lit.[21] $[\alpha]_D^{20} = -5.8$ ($c = 0.18$ in H$_2$O)]; ^{1}H NMR (500 MHz, D$_2$O): $\delta = 4.59$ (m, 1H), 3.87 (t, $^3J =$ 7.3 Hz, 1H), 3.84 (t, $^3J = 8.5$ Hz, 1H), 3.79 (A of AB system, $^3J = 11.7$, 3.7 Hz, 1H), 3.64 (B of AB system, $J = 11.8$, 6.7 Hz, 1H), 3.45 (q, $^3J = 7.3$, 7.2 Hz, 1H), 3.05 (A of AB system, $^3J = 11.7$, 3.0 Hz, 1H), 2.97 (B of AB system, $^3J = 11.8$, 4.5 Hz, 1H), 2.82 (m, 1H), 2.09 (m, 1H), 2.00 ppm (m, 1H); ^{13}C NMR (101 MHz, D$_2$O): $\delta = 82.6$, 79.9, 74.6, 72.7, 68.2, 64.4, 64.2, 40.1 ppm; ESI-TOF: m/z calcd for $[M+H]^+$ C$_8$H$_{16}$NO$_4$: 190.1079; found 190.1079.

(1S,2S,3S,7S,7aS)-1,2,7-Trihydroxy-3-(hydroxymethyl)pyrrolizine **(9i)**: The title compound was prepared by the General Procedure described above (26 mg, 35% from the aldol adduct). $[\alpha]_D^{22} = +17.9$ ($c = 1.7$ in H_2O) (the specific rotation found for this compound or its enantiomer was $[\alpha]_D^{22} = +11.6$ ($c = 0.37$ in H_2O)[25]); ^{1}H NMR (500 MHz, D_2O): $\delta = 4.35$ (dt, $^3J = 4.9$, 2.6 Hz, 1H), 3.78 (A of AB system, $^3J = 11.8$, 3.8, 1H), 3.76 (t, $^3J = 8.3$ Hz, 1H), 3.72 (t, $^3J = 8.2$ Hz, 1H), 3.64 (B of AB system, $^3J = 11.7$, 6.2 Hz, 1H), 3.10 (m, 1H), 3.04 (dd, $^3J = 7.9$, 1.9 Hz, 1H), 2.90 (m, 1H), 2.70 (m, 1H), 2.08 (m, 1H), 1.78 ppm (m, 1H); ^{13}C NMR (101 MHz, D_2O): $\delta = 80.3$, 78.7, 77.6, 76.5, 70.8, 65.0, 54.4, 34.1 ppm; ESI-TOF: m/z calcd for $[M+H]^+$ $C_8H_{16}NO_4$: 190.1079; found 190.1078.

(1S,2S,3R,7S,7aS)-1,2,7-Trihydroxy-3-(hydroxymethyl)pyrrolizine **(9j)**: The title compound was prepared by the General Procedure described above (10 mg, 14% from the aldol adduct). $[\alpha]_D^{22} = +14.2$ ($c = 0.8$ in H_2O) (lit.[23] $[\alpha]_D = +33.0$ ($c = 0.1$ in H_2O), hydrochloride salt); ^{1}H NMR (500 MHz, D_2O): $\delta = 4.35$ (m, 1H), 4.17 (m, 2H), 3.95 (m, 2H), 3.44 (br s, 1H), 3.23 (m, 2H), 3.07 (m, 1H), 2.25 (m, 1H), 1.80 ppm (m, 1H); ^{13}C NMR (101 MHz, D_2O): $\delta = 81.3$ (2C), 80.6, 76.2, 67.6, 58.7, 48.9, 35.8. ESI-TOF: m/z calcd for $C_8H_{16}NO_4$ $[M+H]^+$: 190.1079; found 190.1077.

Enzymatic inhibition assays: Commercial glycosidase solutions were prepared with the appropriate buffer and incubated in 96-well plates at 37 °C without (control) or with inhibitor (1.6 mM to 4.2 nM) for 3 min for α-D-glucosidase, β-D-glucosidase, α-D-mannosidase, α-L-rhamnosidase and α-L-fucosidase and for 5 min for β-D-galactosidase. After addition of the corresponding substrate solution, incubations were continued for different time periods—10 min for α-D-glucosidase, 3 min for β-D-glucosidase, 6 min for α-D-mannosidase, 5 min for α-L-rhamnosidase, 7 min for α-L-fucosidase and 16 min for β-D-galactosidase—and were stopped by addition either of Tris solution (50 μL, 1 M) or of glycine buffer (180 μL, 100 mM, pH 10), depending on the enzymatic inhibition assay. The amount of p-nitrophenol formed was determined at 405 nm with the aid of a UV/VIS Spectramax Plus (Molecular Devices Corporation) spectrophotometer. The activity of α-D-glucosidase from rice was determined with p-nitrophenyl α-D-glucopyranoside (1 mM) in sodium acetate buffer (50 mM, pH 5.0). The activity of β-D-glucosidase was determined with p-nitrophenyl β-D-glucopyranoside (1 mM) in sodium acetate buffer (100 mM, pH 5.0). The activity of β-D-galactosidase was determined with p-nitrophenyl β-D-galactopyranoside (1 mM) in sodium phosphate buffer (100 mM, $MgCl_2$ (0.1 mM), pH 7.2). The activity of α-D-mannosidase was determined with p-nitrophenyl α-D-mannopyranoside (1 mM) in sodium acetate buffer (50 mM, pH 5.0). The activity of α-L-rhamnosidase was determined with p-nitrophenyl α-D-rhamnopyranoside (1 mM) in sodium acetate buffer (50 mM, pH 5.0). The activity of α-L-fucosidase was determined with p-nitrophenyl α-D-fucopyranoside (0.15 mM) in sodium acetate buffer (50 mM, pH 5.0). The commercial glycosidase solutions were prepared as follows: α-D-glucosidase $(NH_4)_2SO_4$ suspension (100 μL) in buffer (5 mL); β-D-glucosidase (0.1 mg mL^{-1} buffer); β-D-galactosidase from *Aspergillus orysae* (0.5 mg mL^{-1} buffer); α-L-rhamnosidase (naringinase, 0.3 mg mL^{-1} buffer); α-D-mannosidase $(NH_4)_2SO_4$ suspension (25 μL) in buffer (10 mL); β-D-galactosidase from bovine liver (0.1 mg mL^{-1} buffer); α-L-fucosidase $(NH_4)_2SO_4$ suspension (33 μL) in buffer (10 mL).

Kinetics of inhibition: The nature of the inhibition against enzymes and the K_i values were determined from Lineweaver–Burk plots.

Rat intestinal disacharidases

Animals: Adult male Sprague–Dawley rats weighing 200 g ($n = 2$, Harlan Ibèrica, Barcelona, Spain) were housed in cages ($n = 2$/cage) under controlled conditions of a 12 h light/dark cycle, with a temperature of 22 ± 3 °C and a relative humidity of 40–70%. Rats were fed on a standard diet (Panlab A04, Panlab, Barcelona, Spain) and water ad libitum. Handling and sacrificing of the animals were in full accordance with the European Community guidelines for the care and management of laboratory animals and the pertinent permission was obtained from the CSIC Subcommittee of Bioethical issues (permit number: CTQ2009–07359). Rats were fasted overnight and then anesthetised by intramuscular injection of ketamine hydrochloride (0.1%, v/weight of rat, Imalgene 1000, Merial Laboratorios S.A., Barcelona, Spain) and xylacine (0.01%, v/weight of rat, Rompun 2%, Química Farmacéutica S.A., Barcelona, Spain)

Preparation of gut mucosal suspension: The small intestine was removed, and carefully divided into duodenum, jejunum and ileum. The jejunum was washed with ice-cold isotonic saline and opened lengthwise, and the mucosa was scraped off with a microscope slide. The jejunum mucosa was stored at −80 °C. The samples were diluted with ice-cold isotonic saline (50 mg mucosa mL^{-1}) and homogenised with a 2 mL glass homogeniser.

Assay of disacharidase activity: Disacharidase, that is, sucrase, lactase, maltase and trehalase, activities in the homogenised jejunum mucosa were determined by the method of Dalqhvist.[45] Enzyme activity (μmol of substrate hydrolysed per hour) were normalised to protein content as evaluated by Bradford's method.[46] The disaccharide substrates, sucrose, lactose, maltose and trehalose, were purchased at the highest purity available (Sigma Chemical Co.). Substrates and inhibitors were prepared in distilled water. The concentrations used in the assay were 0.02 M for the disaccharides and a range from 2 mM down for the inhibitors. The homogenised mucosa was diluted four times for the sucrose and trehalase assays, once for the lactase assay and 25 times for the maltase activity and protein determination assays. Inhibitors and suitably diluted homogenised mucosa were preincubated for 30 min at 37 °C. The reaction was then carried out by the addition of the substrate in phosphate buffer (pH 6.8). Substrate, inhibitor and homogenised mucosa were incubated together for 30 min at 37 °C and under agitation (250 rpm). The reaction was terminated by the addition of Tris-glucose oxidase-peroxidase reagent (Tris (0.5 M), 4-hydroxybenzoic acid (10 mM), 4-aminoantipyrine (0.4 mM), glucose oxidase (1480 UIL^{-1}), peroxidase (250 UIL^{-1}), pH 7.3). Glucose is transformed into gluconic acid and hydrogen peroxide by glucose oxidase. Peroxidase catalyses the combination of hydrogen peroxide with 4-aminoantipiryne, generating a stable and coloured compound. After a further incubation of 2 h this product was measured spectrophotometrically at 505 nm.

Computational methods: Conformational searches on aldol adduct derivatives were conducted as previously described[4,6,47] with use of the program MOE (v. 2008.10, Chemical Computing Group, Montreal). The implemented MMFF94x force field, a modified version of the MMFF94s force field,[48] was used for energy calculations. Electrostatic interactions were approximated by Generalised Born/Volume Integral (GB/VI) methodology[49] without cutoffs. A systematic conformational search in which every non-terminal single bond from a starting initially optimised structure was rotated in 60–120° steps was run. The conformations generated for each compound were then minimised and ranked by energy. To confirm the natures of the lowest-energy conformers determined, a subsequent stochastic conformational search in which the conformational space of the molecules was explored by random rotation of bonds and simultaneous Cartesian perturbation was run. The conformations thus generated were minimised and checked to determine whether or not they were duplicates, within a RMS tolerance (0.1 Å), of previously generated conformations. The process was finished when the number of failures to find new conformations exceeded a large enough number (1000) of attempts.

Protein–substrate simulations were conducted with the Schrödinger Suite 2009 package (Schrödinger, LLC, New York) through its graphical interphase Maestro (Maestro, version 9.0, Schrödinger, LLC, New York, NY, 2009). The program Impact (Impact, version 5.5, Schrödinger, LLC, New York, NY, 2005) with its default OPLS 2005 force field, a modified version of the OPLS-AA force field,[50] and GB/SA water solvation conditions[51] were used for all energy calculations. Coordinates of *E. coli* fuculose-1-phosphate aldolase in complexation with phosphoglycolohydroxamate (PGH) and of the F131A mutant[9,14] were obtained from the Protein Data Bank[52] at Brookhaven National Laboratory (entries 4FUA and 1DZW). The C-terminal tail (residues 206–215), which is absent in these structures, was modelled as previously described[4] and included in all subsequent simulations. The structure of FucA F206 A was generated by mutating the wild type protein in silico. Prior to any simulation, protein structures were prepared with the aid of the Protein Preparation Wizard included in Maestro to remove solvent molecules and ions, with addition of hydrogens, setting of protonation states and minimisation of the energy through the use of the OPLS force field. The structure of fu-

culose-1-phosphate bound into the active centre of the FucA wild type was modelled on the basis of the coordinates of PGH and a model of bound L-lactaldehyde.[15] Aldol adducts derived from *N*-Cbz-prolinal were modelled by starting from the coordinates of PGH and by manual placing of the Cbz phenyl group in the cavities generated by the F131A or F206A mutations. The structures of the protein–substrate complexes were minimised by first applying constraints to the protein (force constant $= 100.00$ kcal Å^{-2} mol^{-1}) to avoid large changes in its structure and afterwards allowing free movement of the whole system either until a gradient < 0.01 kcal mol$^{-1}\text{Å}^{-1}$ was reached or for a maximum of 2000 cycles. The structures were then subjected to 200 ps of molecular dynamics (1 fs step) under the NVT ensemble at 298.16 K, with use of implicit solvent conditions (GBSA) and a force constant of 100 kcal Å^{-2} mol^{-1} to restrain the protein residues more than 15 Å away from the ligand, and were finally minimised again without constraints.

[1] a) R. Mahrwald, *Modern Aldol Reactions, Vol. 1: Enolates, Organocatalysis, Biocatalysis and Natural Product Synthesis*, Wiley-VCH, Weinheim, **2004**, p. 335; b) R. Mahrwald, *Modern Aldol Reactions, Vol. 2: Metal Catalysis*, Wiley-VCH, Weinheim, **2004**, p. 335; c) S. M. Dean, W. A. Greenberg, C.-H. Wong, *Adv. Synth. Catal.* **2007**, *349*, 1308–1320; d) W.-D. Fessner in *Biocatalytic C—C Bond Formation in Asymmetric Synthesis* (Eds.: D. Enders, K.-E. Jaeger), Wiley-VCH, Weinheim, **2007**, pp. 351–375.

[2] W. D. Fessner, G. Sinerius, *Angew. Chem.* **1994**, *106*, 217–220; *Angew. Chem. Int. Ed. Engl.* **1994**, *33*, 209–212.

[3] W.-D. Fessner, C. Walter, *Top. Curr. Chem.* **1997**, *186–193*, 97–194.

[4] L. Espelt, J. Bujons, T. Parella, J. Calveras, J. Joglar, A. Delgado, P. Clapés, *Chem. Eur. J.* **2005**, *11*, 1392–1401.

[5] L. Espelt, T. Parella, J. Bujons, C. Solans, J. Joglar, A. Delgado, P. Clapés, *Chem. Eur. J.* **2003**, *9*, 4887–4899.

[6] J. Calveras, M. Egido-Gabás, L. Gómez, J. Casas, T. Parella, J. Joglar, J. Bujons, P. Clapés, *Chem. Eur. J.* **2009**, *15*, 7310–7328.

[7] J. Calveras, J. Casas, T. Parella, J. Joglar, P. Clapés, *Adv. Synth. Catal.* **2007**, *349*, 1661–1666.

[8] A. Bolt, A. Berry, A. Nelson, *Arch. Biochem. Biophys.* **2008**, *474*, 318–330.

[9] A. C. Joerger, C. Gosse, W.-D. Fessner, G. E. Schulz, *Biochemistry* **2000**, *39*, 6033–6041.

[10] At 4°C the rate of DHAP degradation was minimised and sometimes the conversions to aldol adducts were highly enhanced; see reference [12].

[11] In all experiments conducted thus far the amount of biocatalyst employed in synthetic experiments with *N*-Cbz-amino aldehydes was adjusted to the amount (i.e., mg) of FucA wild type used rather than to the activities on Fuc1P, due to the disparate values of activity observed with this substrate.

[12] T. Suau, G. Alvaro, M. D. Benaiges, J. Lopez-Santín, *Biotechnol. Bioeng.* **2006**, *93*, 48–55.

[13] We were not able to separate the *anti/syn* diastereomers of the aldol adduct (5S)-**4a** on the preparative HPLC. Therefore this compound was assayed as a diastereomeric mixture 1:1 *anti/syn*.

[14] M. K. Dreyer, G. E. Schulz, *Acta Crystallogr. Sect. D* **1996**, *52*, 1082–1091.

[15] A. C. Joerger, C. Mueller-Dieckmann, G. E. Schulz, *J. Mol. Biol.* **2000**, *303*, 531–543.

[16] a) J. R. Liddell, *Nat. Prod. Rep.* **2001**, *18*, 441–447; b) L. Rambaud, P. Compain, O. R. Martin, *Tetrahedron: Asymmetry* **2001**, *12*, 1807–1809; c) I. Izquierdo, M. T. Plaza, F. Franco, *Tetrahedron: Asymmetry* **2002**, *13*, 1581–1585; d) I. Izquierdo, M. T. Plaza, F. Franco, *Tetrahedron: Asymmetry* **2003**, *14*, 3933–3935; e) I. Izquierdo, M. T. Plaza, R. Robles, C. Rodriguez, A. Ramirez, A. J. Mota, *Eur. J. Org. Chem.* **1999**, 1269–2174; f) I. Izquierdo, M. T. Plaza, J. A. Tamayo, *Tetrahedron: Asymmetry* **2004**, *15*, 3635–3642; g) I. Izquierdo, M. T. Plaza, J. A. Tamayo, D. L. Re, F. Sánchez-Cantalejo, *Synthesis* **2008**, 1373–1378; h) I. Izquierdo, M. T. Plaza, V. Yanez, *Tetrahedron* **2007**, *63*, 1440–1447; i) F. Cardona, E. Faggi, F. Liguori, M. Cacciarini, A. Goti, *Tetrahedron Lett.* **2003**, *44*, 2315–2318; j) T. J. Donohoe, M. D. Cheeseman, T. J. C. O'Riordan, J. A. Kershaw, *Org. Biomol. Chem.* **2008**, *6*, 3896–3898; k) L. Chabaud, Y. Landais, P. Renaud, *Org. Lett.* **2005**, *7*, 2587–2590; l) J. A. Tamayo, F. Franco, D. Lo Re, F. Sanchez-Cantalejo, *J. Org. Chem.* **2009**, *74*, 5679–5682.

[17] I. Izquierdo, M. T. Plaza, F. Franco, *Tetrahedron: Asymmetry* **2004**, *15*, 1465–1469.

[18] I. Izquierdo, M. T. Plaza, R. Robles, F. Franco, *Tetrahedron: Asymmetry* **2001**, *12*, 2481–2487.

[19] I. Izquierdo, M. T. Plaza, J. A. Tamayo, F. Sanchez-Cantalejo, *Tetrahedron: Asymmetry* **2007**, *18*, 2211–2217.

[20] I. Izquierdo, M. T. Plaza, J. A. Tamayo, V. Yanez, D. Lo Re, F. Sanchez-Cantalejo, *Tetrahedron* **2008**, *64*, 4613–4618.

[21] D. Koch, S. Maechling, S. Blechert, *Tetrahedron* **2007**, *63*, 7112–7119.

[22] J.-B. Behr, A. Erard, G. Guillerm, *Eur. J. Org. Chem.* **2002**, 1256–1262.

[23] D. Chikkanna, O. V. Singh, S. B. Kong, H. Han, *Tetrahedron Lett.* **2005**, *46*, 8865–8868.

[24] a) R. J. Nash, L. E. Fellows, J. V. Dring, G. W. J. Fleet, A. E. Derome, T. A. Hamor, A. M. Scofield, D. J. Watkin, *Tetrahedron Lett.* **1988**, *29*, 2487–2490; b) A. Kato, I. Adachi, M. Miyauchi, K. Ikeda, T. Komae, H. Kizu, Y. Kameda, A. A. Watson, R. J. Nash, M. R. Wormald, *Carbohydr. Res.* **1999**, *316*, 95–103.

[25] R. J. Nash, L. E. Fellows, J. V. Dring, G. W. J. Fleet, A. Girdhar, N. G. Ramsden, J. M. Peach, M. P. Hegarty, A. M. Scofield, *Phytochemistry* **1990**, *29*, 111–114.

[26] N. Asano, H. Kuroi, K. Ikeda, H. Kizu, Y. Kameda, A. Kato, I. Adachi, A. A. Watson, R. J. Nash, G. W. J. Fleet, *Tetrahedron: Asymmetry* **2000**, *11*, 1–8.

[27] T. Yamashita, K. Yasuda, H. Kizu, Y. Kameda, A. A. Watson, R. J. Nash, G. W. J. Fleet, N. Asano, *J. Nat. Prod.* **2002**, *65*, 1875–1881.

[28] a) *From Synthesis Iminosugars to Therapeutic Applications* (Eds.: P. Compain, O. R. Martin), Wiley, New York, **2007**, p. 467; c) J. Churruca, L. Vigil, E. Luna, J. Ruiz-Galiana, M. Varela, *Diabete Metab.* **2008**, *1*, 3–11; d) A. Esteghamati, O. Khalilzadeh, M. Anvari, M. S. Ahadi, M. Abbasi, A. Rashidi, *Arch. Med. Res.* **2008**, *39*, 803–808; e) K. Kim, S. H. Yun, B. Y. Choi, M. K. Kim, *Br. J. Nutr.* **2008**, *100*, 576–584; f) L. R. Reynolds, *Nutraceuticals, Glycemic Health Type 2 Diabetes*, Wiley-Blackwell, New York, **2008**, pp. 65–86.

[29] O. Affolter, A. Baro, W. Frey, S. Laschat, *Tetrahedron* **2009**, *65*, 6626–6634.

[30] a) A. Kato, E. Kano, I. Adachi, R. J. Molyneux, A. A. Watson, R. J. Nash, G. W. J. Fleet, M. R. Wormald, H. Kizu, K. Ikeda, N. Asano, *Tetrahedron: Asymmetry* **2003**, *14*, 325–331; b) T. J. Donohoe, R. E. Thomas, M. D. Cheeseman, C. L. Rigby, G. Bhalay, I. D. Linney, *Org. Lett.* **2008**, *10*, 3615–3618.

[31] S. Desvergnes, S. Py, Y. Vallee, *J. Org. Chem.* **2005**, *70*, 1459–1462.

[32] N. Asano, K. Ikeda, L. Yu, A. Kato, K. Takebayashi, I. Adachi, I. Kato, H. Ouchi, H. Takahata, G. W. J. Fleet, *Tetrahedron: Asymmetry* **2005**, *16*, 223–229.

[33] A. E. Stutz, *Iminosugars as Glycosidase Inhibitors: Nojirimycin and Beyond*, Wiley-VCH, Weinheim, **1999**, p. 397.

[34] A. L. Concia, C. Lozano, J. A. Castillo, T. Parella, J. Joglar, P. Clapés, *Chem. Eur. J.* **2009**, *15*, 3808–3816.

[35] J. A. Castillo, J. Calveras, J. Casas, M. Mitjans, M. P. Vinardell, T. Parella, T. Inoue, G. A. Sprenger, J. Joglar, P. Clapés, *Org. Lett.* **2006**, *8*, 6067–6070.

[36] *Evaluation of Enzyme Inhibitors in Drug Discovery: A Guide to Medicinal Chemists and Pharmacologists* (Ed.: R. A. Copeland), Wiley-Interscience, New York, **2005**, p. 296.

[37] S.-H. Jung, J.-H. Jeong, P. Miller, C.-H. Wong, *J. Org. Chem.* **1994**, *59*, 7182–7184.

[38] W. D. Fessner, A. Schneider, O. Eyrisch, G. Sinerius, J. Badia, *Tetrahedron: Asymmetry* **1993**, *4*, 1183–1192.

[39] L. Vida, PhD Thesis, Universitat Autonoma de Barcelona (Spain), **2006**.

[40] Z. Q. Zhang, A. G. Marshall, *J. Am. Soc. Mass Spectrom.* **1998**, *9*, 225–233.

[41] L. Vidal, O. Durany, T. Suau, P. Ferrer, M. D. Benaiges, G. Caminal, *J. Chem. Technol. Biotechnol.* **2003**, *78*, 1171–1179.

[42] O. Durany, G. Caminal, C. de Mas, J. Lopez-Santin, *Process Biochem.* **2004**, *39*, 1677–1684.

[43] L. Espelt, P. Clapés, J. Esquena, A. Manich, C. Solans, *Langmuir* **2003**, *19*, 1337–1346.

[44] J. R. Luly, J. F. Dellaria, J. J. Plattner, J. L. Soderquist, N. Yi, *J. Org. Chem.* **1987**, *52*, 1487–1492.

[45] A. Dahlqvist, *Anal. Biochem.* **1964**, *7*, 18–25.

[46] M. M. Bradford, *Anal. Biochem.* **1976**, *72*, 248–254.

[47] J. Calveras, J. Bujons, T. Parella, R. Crehuet, L. Espelt, J. Joglar, P. Clapés, *Tetrahedron* **2006**, *62*, 2648–2656.

[48] a) T. A. Halgren, *J. Comput. Chem.* **1999**, *20*, 730–748; b) T. A. Halgren, *J. Comput. Chem.* **1999**, *20*, 720–729.

[49] P. Labute, *J. Comput. Chem.* **2008**, *29*, 1693–1698.

[50] W. L. Jorgensen, D. S. Maxwell, J. TiradoRives, *J. Am. Chem. Soc.* **1996**, *118*, 11225–11236.

[51] W. C. Still, A. Tempczyk, R. C. Hawley, T. Hendrickson, *J. Am. Chem. Soc.* **1990**, *112*, 6127–6129.

[52] H. M. Berman, J. Westbrook, Z. Feng, G. Gilliland, T. N. Bhat, H. Weissig, I. N. Shindyalov, P. E. Bourne, *Nucleic Acids Res.* **2000**, *28*, 235–242.